Ref.TH.2113-CERN

INADEQUACY OF THE SPECTATOR MODEL IN DEUTERON BREAK-UP INDUCED BY HIGH ENERGY HADRONS

G. Alberi

Istituto di Fisica Teorica and INFN, Miramare, Trieste
and
CERN -- Geneva

V. Hepp

CERN -- Geneva

L.P. Rosa and Z.D. Thomé

Centro de Ciencias Matematicas e do Naturezas,
Instituto de Fisica, Universidad Federal do
Rio de Janeiro

A B S T R A C T

We discuss the experimental features of the spectator distribution in high energy reactions on deuterons and we compare them with the quantitative and qualitative predictions of various theoretical models. We find that only a particular type of meson exchange can explain the relative channel dependence. Extending our analysis to the case of a hyperon and a nucleon in the final state, we find it more practical to look at this effect from a different point of view, namely introducing isobars in the final scattering state.

Ref.TH.2113-CERN
19 December 1975

1. INTRODUCTION

Since a few years, there is experimental evidence that the impulse approximation is not valid for deuteron break-up reactions at high energies: this evidence shows up in the comparison of the so-called "spectator" distribution with the theoretical probability $P(p)$ of finding a nucleon p in the deuteron. If this function is normalized to the low momentum part of the experimental spectrum, the predicted high momentum tail is in clear disagreement with the experimental data above 300 MeV/c. This comparison was presented for the first time in the literature by Perdrisat et al. [1] who performed a counter experiment for the reaction $pD \to ppn$. Immediately afterwards Brunt et al. [1] published the report of a bubble chamber experiment, where they studied one- and two-pion production with incident protons; in order to explain the discrepancy in the tail of the "spectator" distribution, they suggest that at high momenta the "spectators" are emitted simply according to the phase space distribution, multiplied by an experimentally determined numerical factor.

Another suggestion, raised in the literature [2], was that the wave function of the deuteron, consistent with nucleon-nucleon scattering data [3], is not correct in the high momentum region. This hypothesis is not easy to accept, because the theoretical wave functions are consistent with elastic electron scattering data for comparable momentum transfers $(q = 2 \div 4p)$. Furthermore, if this were true, the "spectator" distribution should be less channel-dependent than indicated by experimental data. Actually, as shown in Section 3, there is a very rich structure in the channel dependence which cannot be explained by a simple spectator model, even including the interaction of the nucleons in the final state.

In Section 4 we discuss the possible corrections to the spectator model and conclude that only the inclusion of the mesonic degree of freedom [4], in the final state of the nucleon pair, can explain the relative channel dependence. Furthermore, we find that for a hyperon and a nucleon in the final state, the additional degree of freedom -- given by the $\Sigma\Lambda$ conversion -- has to be taken into account.

In Section 2 we discuss the kinematics and the "misidentification" effect which occurs whenever two nucleons are present in the final state.

2. "SPECTATOR" DISTRIBUTION

When two nucleons are present in the final state, the "spectator" distribution is by definition the momentum spectrum of the slower nucleon emitted by the broken deuteron. This definition has a clear physical

meaning when we study large angle scattering and production; when we consider small angles, and therefore small recoils of the active nucleon, the problem of "misidentification" of the spectator arises. In other words, it is not clear whether we have identified the spectator with the above choice. In Fig. 1 we show a kinematical configuration where the above criterion fails to identify the spectator: that is, when the momentum transfer is of the order of the Fermi momentum, the recoil momentum may be smaller than the spectator momentum. This is not a problem, however, from the theoretical point of view, because we compare the "spectator" distribution with a properly symmetrized single scattering model.

Let us consider a simple process with only three particles in the final state

$$a + b \to c + 1 + 2$$

where a labels the incident projectile and b the deuteron, 1 and 2 the nucleons and c the scattered projectile or the produced particle. The "spectator" distribution is

$$\frac{d\sigma}{dp} = \sum_f \overline{\sum_i} \left\{ |\langle \psi_f(1;2) | \hat{O}(1,2) | \psi_i \rangle|^2 \, \Theta(q_2 - q_1)\, \delta(q_1 - p) + |\langle \psi_f(2;1) | \hat{O}(1,2) | \psi_i \rangle|^2 \, \Theta(q_1 - q_2)\, \delta(q_2 - p) \right\} dV^{(3)} \tag{2.1}$$

where $$\hat{O}(1,2) = (16\pi^3 M)^{1/2} \left[\hat{T}_1 \psi(q_2) + \hat{T}_2 \psi(q_1) \right]$$

and $$\psi(q) = \psi_v(q) + \frac{1}{\sqrt{8}} \left(3(\vec{\sigma}_1 \cdot \hat{q})(\vec{\sigma}_2 \cdot \hat{q}) - \vec{\sigma}_1 \cdot \vec{\sigma}_2 \right) \psi_w(q)$$

$\hat{T}_i$ is the scattering or production operator in the spin and isospin space [5),6)] of the two nucleons, and ψ_i, ψ_f are the initial and final spin and isospin states: q_1 and q_2 are the momenta of the nucleons, $dV^{(3)}$ is the three-body phase space, and M is the deuteron mass.

The above expression is completely symmetric for interchange of the labels 1 and 2, as it should be for identical particles: in actual practice, since $\hat{O}(1,2)$ is symmetric for the exchange of the labels and ψ_i is

antisymmetric, it is sufficient to multiply one of the above expressions by a factor of two. For the charge preserving case, that is for a neutron and a proton in the final state, the two different spectator distributions are distinguished by a different definition of the isospin space for the neutron distribution $\beta(1)\,\alpha(2)$ and for the proton $\alpha(1)\,\beta(2)$ *) in the first term of expression (2.1).

Making assumptions about the elementary amplitude, we can calculate the "spectator" distribution and compare it with the prediction of a naive spectator model, including the effect of the phase space: we call the difference between the two curves the "misidentification" effect.

First of all, we assume that the spin and isospin dependence of the elementary amplitude is given in the most general way by:

$$\hat{T}_i = A + \hat{B}\cdot\vec{\sigma}_i + \vec{C}\cdot\vec{\tau}_i + (\vec{D}\cdot\vec{\tau}_i)(\hat{E}\cdot\vec{\sigma}_i) \qquad (2.2)$$

from which we get the general form for $d\sigma/dp$; at a later stage we make simple assumptions to calculate the effect numerically.

(a) The isospin matrix element of the amplitude $\hat{O}(1,2)$ in the case of <u>charge exchange</u> is given by:

$$\langle I_f | \hat{O}(1,2) | I_i \rangle = \frac{(16\pi^3 M)^{1/2}}{\sqrt{2}} \left[-(C_- + D_- \hat{E}\cdot\vec{\sigma}_1)\,\psi(q_2) + (C_- + D_- \hat{E}\cdot\vec{\sigma}_2)\,\psi(q_1) \right] \qquad (2.3)$$

where $C_- = C_x - i C_y$; $D_- = D_x - i D_y$

Using the sum rules of Appendix A we obtain for the "spectator" distribution

*) $\alpha \equiv \begin{pmatrix} 1 \\ 0 \end{pmatrix}$ and $\beta \equiv \begin{pmatrix} 0 \\ 1 \end{pmatrix}$ as usual.

$$\frac{d\sigma}{dp} = p^2 \int dt\, d\Omega_1\, \Theta(q_2 - q_1)\, \frac{d\sigma(cex)}{dt} \times$$

$$\times \Big\{ \psi_v^2(q_1) + \psi_w^2(q_1) + \psi_v^2(q_2) + \psi_w^2(q_2) -$$

$$- 2R_F(t)\, \Phi(v,w|\vec{q}_1,\vec{q}_2) - 2R_G(t)\, \Psi(v,w|\hat{E},\vec{q}_1,\vec{q}_2) \Big\} \tag{2.4}$$

with

$$\Phi(v,w|\vec{q}_1,\vec{q}_2) = \psi_v(q_1)\psi_v(q_2) + \tfrac{1}{2}\left(3(\hat{q}_1\cdot\hat{q}_2)^2 - 1\right)\psi_w(q_1)\psi_w(q_2)$$

$$\Psi(v,w|\hat{E},\vec{q}_1,\vec{q}_2) = \psi_v(q_1)\psi_v(q_2) - \sqrt{2}\left((\hat{E}\cdot\hat{q}_1)^2 - \tfrac{1}{3}\right)\psi_w(q_1)\psi_v(q_2)$$

$$- \sqrt{2}\left((\hat{E}\cdot\hat{q}_2)^2 - \tfrac{1}{3}\right)\psi_v(q_1)\psi_w(q_2) + \Big[\tfrac{3}{2}\left(\hat{E}\cdot(\hat{q}_1\times\hat{q}_2)\right)^2$$

$$+ \tfrac{1}{2}\left((\hat{E}\cdot\hat{q}_1)^2 + (\hat{E}\cdot\hat{q}_2)^2\right) - \tfrac{2}{3}\Big]\psi_w(q_1)\psi_w(q_2)$$

where

$$R_F(t) = |F_{cex}|^2 \Big/ \frac{d\sigma(cex)}{dt} \quad \text{and} \quad R_G(t) = |G_{cex}|^2 \Big/ \frac{d\sigma(cex)}{dt}$$

(F,G are non-spin-flip and spin-flip amplitudes normalized to $R_F + R_G = 1$).

(b) For the <u>charge preserving case</u> the isospin matrix element is

$$\langle I_f | \hat{O}(1,2) | I_i \rangle = \frac{(16\pi^3 M)^{1/2}}{\sqrt{2}} \Big[(f_1 + g_1\, \hat{n}\cdot\vec{\sigma}_1)\psi(q_2) + (f_2 + g_2\, \hat{n}\cdot\vec{\sigma}_2)\psi(q_1) \Big] \tag{2.5}$$

f_i and g_i being related to A,B,C,D [6].

In (2.5) and (2.2) we have assumed that the spin-flip amplitude can be separated in a scalar part and in a versor. This is rigorously true for most cases considered here such as pseudoscalar meson nucleon scattering and photoproduction. For other cases such as nucleon-nucleon scattering, where the ansatz is not true, the qualitative features of the result should not change.

The "spectator" distribution is calculated using again the sum rules of Appendix A:

$$\frac{d\sigma}{dp} = p^2 \int dt\, d\Omega_1\, \Theta(q_2 - q_1)\, \delta(q_1 - p)\, \frac{d\sigma_2}{dt} \Big\{ \psi_v^2(q_1) + \psi_\omega^2(q_1) +$$

$$+ R_\sigma(t) \left[\psi_v^2(q_2) + \psi_\omega^2(q_2) \right] + 2 R_f(t)\, \Phi(v,\omega \mid \vec{q}_1, \vec{q}_2)$$

$$+ 2 R_g(t)\, \Psi(v,\omega \mid \hat{n}, \vec{q}_1, \vec{q}_2) + 2 R_{fg}(t)\, \Xi(\omega \mid \hat{n}, \hat{q}_1, \hat{q}_2) \Big\} \tag{2.6}$$

with

$$\Xi(\omega \mid \hat{n}, \hat{q}_1, \hat{q}_2) = \frac{3}{2} (\hat{q}_1 \cdot \hat{q}_2)\, \hat{n} \cdot (\hat{q}_1 \times \hat{q}_2)\, \psi_\omega(q_1)\, \psi_\omega(q_2)$$

and

$$R_\sigma(t) = \frac{d\sigma_1}{dt} \Big/ \frac{d\sigma_2}{dt}$$

$$R_f(t) = \mathrm{Re}\left[F_1^* F_2 \right] / d\sigma_2/dt$$

$$R_g(t) = \mathrm{Re}\left[G_1^* G_2 \right] / d\sigma_2/dt$$

$$R_{fg}(t) = -\mathrm{Im}\left[G_1^* F_2 - G_2^* F_1 \right] / d\sigma_2/dt$$

(F_i, G_i are non-spin-flip and spin-flip amplitudes normalized in the same way as for the charge exchange case.)

Before actually calculating the "misidentification" effect, we make some considerations on the phase space integration in (2.5) and (2.6). These considerations are independent from the expression inside the curly brackets and hold also for the unambiguous cases like $K^- D \to \Sigma^- \pi^+ n_s$. Because of energy conservation there are x kinematically forbidden areas for Ω_1, and even in the unambiguous cases the momentum spectrum of the spectator cannot be identified with the momentum distribution in the deuteron.

The simplest kinematical condition is given by

$$s_{32} = (q_3 + q_2)^2 \geq (m_3 + m_2)^2 \quad *) \tag{2.7}$$

where the equal sign corresponds to the situation where particles 3 and 2 are stopped in the laboratory system and all the kinetic energy is concentrated in particle 1. Using energy and momentum conservation, s_{32} can be expressed as a function of the modulus and the angle of q_1:

$$\begin{aligned} s_{32} = (q_a + q_b - q_1)^2 = m_a^2 + m_b^2 + m_1^2 \\ + 2m_b E_a - 2m_b E_1 - 2E_a E_1 + 2\vec{q}_a \cdot \vec{q}_1 \end{aligned} \tag{2.8}$$

where the index a refers to the incident projectile and b to the deuteron. In the above expression we can neglect the binding energy of the deuteron and terms of higher order than $q_1^2/(2m^2)$: for $m_a = m_3$ (quasi-elastic scattering) we find that the condition (2.7) is equivalent to the following limit for $\cos(\hat{q_1 q_a})$

$$\cos(\hat{q_1 q_a}) \geq -\frac{m}{q_1}\frac{T_a}{q_a} + \frac{q_1}{q_a}\left(1 + \frac{E_a}{m}\right) \tag{2.9}$$

where T_a is the kinetic energy of the incident particle. For $m_3 > m_a$, we have to add to the right-hand side a positive term $(m_3^2 - m_a^2)/(2q_a q_1)$ which gives an additional restriction to the allowed physical region. In addition to (2.7) we have an upper limit for $s_{12} = (q_1 + q_2)^2$, depending on $t = (q_a - q_c)^2$ [7], which at high energies is more restrictive than (2.7) because s_{12} is very close to the lower limit $(s_{12})_{min} = 4m^2$ for small values of t, where all the cross-section is concentrated for dynamical reasons.

These kinematical restrictions are present, irrespective of whether the spectator is ambiguous or uniquely identified. In the ambiguous case the condition

$$q_1 < q_2 \tag{2.10}$$

which defines the spectator, gives rise to further distortions of the spectrum.

---

*) This condition was studied in the case of deep inelastic electron scattering in Ref. 2).

Qualitatively the effect (2.10) can be understood for the particular case where $\vec{q}_1$ is collinear with the momentum transfer $\vec{\Delta} = \vec{q}_a - \vec{q}_3 = \vec{q}_1 + \vec{q}_2$, hence $\vec{q}_2$ is also collinear with $\vec{\Delta}$. For this case, if q_1 is larger than $\Delta/2$, q_2 is bound to be smaller than q_1: then in the whole cone around $\vec{\Delta}$, q_1 cannot be larger than $\Delta/2$. To show quantitatively how much the "spectator" distribution is distorted by the above condition, we must use a computer programme which performs the integration over the phase space of formula (2.1) with the condition (2.10).

The calculation was made for the particular case $K^+D \to K^{*o}pp$ at 2.0 GeV/c, which we will consider later on in more detail. We assume that the elementary amplitude is pure spin flip and real, as it would be for a pure π exchange. The cross-section was parametrized as the sum of two exponentials

$$\left.\frac{d\sigma}{dt}\right|_{K^+n \to K^{o*}p} = B_1 e^{b_1 t} + B_2 e^{b_2 t} \qquad (2.11)$$

where $B_{1,2}$ are 8.1, 1.6 mb/(GeV/c)^2 and $b_{1,2}$ are 8, 2.5 (GeV/c)^2, consistent with the data of Islam at 2.2 GeV/c [8].

In order to show the effect of the phase space, we plot in Fig. 2 the probability function (crosses)

$$\frac{d\sigma}{dp} = \mathcal{P}(p) \int \frac{d\sigma}{dt}\, d|t| \qquad (2.12)$$

where

$$\mathcal{P}(p) = 4\pi p^2 \left(\gamma_v^2(p) + \gamma_\omega^2(p)\right)$$

and we compare with the result of the integration (2.4) without the condition (2.10) (open circles):

$$\frac{d\sigma}{dp} = \frac{\mathcal{P}(p)}{4\pi} \int d\Omega_1\, d|t|\, \delta(p - q_1)\, \frac{d\sigma}{dt} \qquad (2.13)$$

As can be seen from Fig. 2a, the kinematical limits reduce the integrated cross-section above 250 MeV/c by about a factor 2. The inclusion of the condition (2.10) reduces the cross-section further by 20%: the "misidentification" effect produces a small enhancement in the region around

300 MeV/c, and a slight suppression in the low momentum region, but it does not change qualitatively the predictions of the spectator model. In Fig. 2b we compare the results of (2.6) with symmetrization (solid curve) and without symmetrization (dashed curve) for the ideal case of purely non-spin-flip amplitudes and with $R_\sigma = 4$, $R_{\hat{f}} = 2$. The ratio R_σ and the parametrization of the cross-section

$$\frac{d\sigma_2}{dt} = c\, e^{\gamma t}$$

with $c = 2.7$ mb/(GeV/c)^2 and $\gamma = 2$ (GeV/c)$^{-2}$, were inspired by the experimental data for $K^+D \to K^{*+}n\,(p_s)$ at 1.4 GeV/c [9]. The figure shows that the effect is very small on the low momentum part - of the order of 3% for $p < 250$ MeV/c; on the high momentum part, the enhancement from the integral above 250 MeV/c is of the order of 40%. Even in this extreme case there is no drastic effect of "misidentification".

3. CHANNEL DEPENDENCE OF THE "SPECTATOR" DISTRIBUTION

The channel dependence of the "spectator" distribution was discovered by Benson [10]. His experimental observations were reported by Musgrave [11] and are still the most complete evidence published for the channel dependence. His procedure consists in displaying for various processes the fraction f of events with a "spectator" of momentum greater than 250 MeV/c. In Fig. 3 we show his results for reactions of the type $\pi^+D \to X^0pp$, with X^0 being a neutral pionic resonance. The most striking feature is the large difference (a factor of 4) between η^0 and f^0 production. Furthermore, he considers the behaviour of f as a function of the number of pions in the final state and he finds that it can be approximated by a straight line: that is, f is increasing linearly with the number of pions (Fig. 4). Even for incident protons [1], the parameter needed in the phase space model of Ref. 1) to fit the high momentum excess is larger for the channel $pp\,\pi^+\pi^-(n_s)$ than for $pp\,\pi^-(p_s)$. In this last experiment, the forward backward asymmetry in the "spectator" angle increases as well, showing a correlation of these two experimental facts.

For incident K mesons [9),12)], $f_\bullet$ is channel dependent; as shown in Fig. 5, the behaviour of f for K^0 and K^{0*} goes in the same direction as for π^0 and ρ^0 in the Benson data, although the absolute value is lower.

The fact that f is considerably different in ρ^0 and K^{0*} production, is very important, as we shall see in the following. From the comparison of the experimental f for the reaction $K^+D \to K^+\pi^-pp$ at $1 \div 1.5$ GeV/c [9] and

at 4.6 GeV/c [12], we see that there is very little energy dependence of the effect. Other comparisons can be done using the same sample of data of Ref. 9) between the channels $K^+D \to K^0\pi^+n(p_s)$ and $K^+D \to K^0\pi^+p(n_s)$: it turns out that f is considerably larger in the first case than in the second.

More recently, a new type of experiment was performed by Aladashvili et al. [13] with incident deuterons in a hydrogen bubble chamber, to get information on np scattering and charge exchange: f was found to be larger for charge exchange than in the charge preserving case, as seen in Fig. 5.

A more detailed way to look at the channel dependence is the plot of f as a function of t: in Fig. 7 we report such dependence for the ρ^0 and f^0 channel for incident π^+, from Benson [10].

One of the most interesting experimental analyses in this field was done recently by Poster and Schlein et al. [14]: they integrated the experimental cross-section $d\sigma/dt\, dm_{pp}$ for the process $K^+D \to K^{0*}pp$ at 2.0 GeV/c in a particular interval of the invariant mass of the two protons. The result was a beautiful structure at small t (Fig. 8), very suggestive of a π meson exchange mechanism. It turns out that the above interval contains the threshold for the process $pp \to \Delta N$.

In this experiment it is shown also that for $m_{pp} \geq 2.09$ GeV the forward backward asymmetry of the "spectator" angular distribution is of opposite sign, as observed before, for instance, by Brunt et al. [1]. This has to do with kinematics since large invariant masses are favoured in the backward direction: this is confirmed by the authors of Ref. 14) who fit the angular distribution, using a spectator model with a modified wave function, in order to fit the "spectator" spectrum.

Instead of using the parameter f, one can compare directly the "spectator" distributions for different reactions with the probability function P(p) (2.12), as reference curve. Even selecting the data with high statistics, the interesting region at high momenta is poorly known, and from the comparison with the probability function or with other data we cannot learn much more than we already know from f. Only at small momenta can one detect some channel dependence: the richest data for $Dp \to ppn$ at 3.3 GeV/c by Aladashvili et al. [13] and for $\gamma D \to \pi^- pp$ by Benz et al. [15] show very good agreement with the probability distribution P(p), as shown in Figs. 9 and 10. Even the spectator spectrum for $\bar{p}D$ annihilation [16] and for the reactions $\pi^+D \to 4\pi pp$ [17] and $K^+D \to K^+\pi^- pp$ [12] show reasonable agreement with P(p) in the low momentum part (Fig. 11):

only from the high statistics curve in $\bar{p}D$ annihilation data, one could state that there is a slight suppression of the experimental spectrum between 100 and 200 MeV/c. The other curves, like Fig. 12 for $K^+D \to K^o pp$ at several energies around 1 GeV/c, show some statistical fluctuations around the theoretical curve. Only for the process $K^-D \to \Sigma$ or Λ π's (n_s) at 3 GeV/c is there a clear shifting of the low momentum peak towards higher momenta, as we can see on Fig. 13. The shifting is confirmed by high statistics data at lower energies [18] for the channel $\Sigma^+\pi^-$, as shown by Fig. 14. A more detailed analysis of the experimental data gives a numerical value of $\sim$ 10 MeV/c for the shifting. For other channels like $\Sigma^-\pi^+$ and $\Lambda\pi^+\pi^-$, this phenomenon is less pronounced.

So while for non-strange hadrons and for the K^+ there is no evidence for any spurious effect in the low momentum part of the spectrum, it seems that for incident K^- the effect is visible even there. Since the effect on the high momentum part is of the same size as for other hadrons, it looks as if the mechanism is of a different nature.

4. CORRECTIONS TO THE SPECTATOR MODEL

In order to discuss as completely as possible the theoretical understanding of the phenomenon, we review all the possible corrections to the spectator model. Qualitative and quantitative predictions are compared with two types of experimental information: the size of the effect in particular cases and the channel dependence.

4.1 Double scattering

The simplest correction to the spectator model is the double collision of the incident particle on two nucleons of the deuteron (Fig. 15a): this effect was calculated by Dean [19] using Glauber theory [20] and it was found to be large at high momenta of the spectator, supporting an interpretation of the excess in terms of double scattering. As later noticed by Alberi, Rosa and Thomè [21], he neglected the D wave of the deuteron and calculated the effect only for "spectators" with transverse momentum. It turns out that the effect is maximum for transverse "spectators" and it decreases going forward or backward, becoming even negative at the extremes of the angular interval. Therefore after integrating over all angles, the result becomes very small and is not comparable with the effect seen in experimental data.

For elastic scattering of hadrons on deuteron, the two nucleons recoil transversely because they have to form the deuteron in the final state; here, although the total momentum transfer is at 90^o, $\vec{q}_1$, $\vec{q}_2$ can be

directed anywhere provided that their sum is transverse. Only if the energy loss of the incident projectile is very small, as for the pD experiment at 19 GeV/c [22], $\vec{q}_1$ and $\vec{q}_2$ have to be transverse as well.

These theoretical considerations rule out the interpretation of the effect as being due to a double scattering. This conclusion is confirmed by a thorough look at the channel dependence (Fig. 5): if the difference between K^{o*} and ρ^o production is suggestive of a double collision, $\sigma_T(\pi N) \sim 1.5\ \sigma_T(KN)$, other comparisons such as charge exchange for π and proton are in contradiction with this assumption.

4.2 Binding correction

The binding diagram of Fig. 15b corresponds to the action of the binding potential of the nucleon pair on the propagation of the hadron; in fact, the lower blob is the nucleon-nucleon scattering amplitude corresponding to the iteration of the potential. The analytic result which we report below is, apart from normalization constants, identical to the formula from multiple scattering theory, derived by Julius [23].

The diagram has already been calculated by Kolybasov and Kondratyuk [24] in the case of elastic scattering, and was shown to suffer almost complete cancellation by the recoil correction of the double scattering for a small range of energies. It is possible to show that a partial cancellation occurs for any energy, provided it is high: this is done in Appendix B and the procedure can easily be generalized to the case of the deuteron break-up. With the notation of Fig. 15a, the double scattering amplitude is *)

$$\hat{T}_D = -\frac{1}{4}\sqrt{\frac{M}{\pi^3}} \int \frac{d^3\eta}{2m\omega} \left[\frac{4(\vec{q}_2-\vec{\eta})\, T_2(\vec{\eta})\, T_1(\vec{\Delta}-\vec{\eta})}{\frac{\vec{K}\cdot\vec{\eta}}{\omega} - \left(\frac{\eta^2}{2\omega} + \epsilon + \frac{(\vec{q}_2-\vec{\eta})^2}{2m} + \frac{q_2^2}{2m}\right) + i\delta} \right.$$

$$\left. + \frac{4(\vec{q}_1-\vec{\eta})\, T_1(\vec{\eta})\, T_2(\vec{\Delta}-\vec{\eta})}{\frac{\vec{K}\cdot\vec{\eta}}{\omega} - \left(\frac{\eta^2}{2\omega} + \epsilon + \frac{(\vec{q}_1-\vec{\eta})^2}{2m} + \frac{q_1^2}{2m}\right) + i\delta} \right] \qquad (4.1)$$

*) The normalization for the T matrix is such that $S_{fi} = \delta_{fi} + i(2\pi)^4 \delta(P_f - P_i) T_{fi}$.

where M is the mass of the deuteron and ϵ its binding energy; m is the nucleon mass and ω the incident energy. As is well known [20], we have to keep the principal value of the propagator here, while its contribution is automatically zero in the elastic scattering case.

The binding diagram is with the notation of Fig. 15b

$$\hat{T}_B = \frac{\sqrt{\pi M}}{2^6 \pi^5 m^2} \int \frac{d^3\xi\, d^3\eta}{2m\omega} \Big[\psi(\xi)\, T_2(\eta)\, T_{NN}\left(\vec{\xi}+\vec{\eta}_{/2}, \vec{q}_2 - \vec{\eta}_{/2}\right) T_1(\vec{\Delta}-\vec{\eta}) \cdot$$

$$\times \left(\eta_{11} - \left[\frac{\eta^2}{2\omega} + \epsilon + \frac{\eta^2}{4m} + \frac{(\vec{\xi}-\vec{\eta}_{/2})^2}{4m}\right]\right)^{-1} \times$$

$$\times \left(\eta_{11} - \left[\frac{(\vec{\eta}-\vec{q}_2)^2}{2m} + \frac{\eta^2}{2\omega} + \frac{\vec{\Delta}\cdot\vec{\eta}}{2\omega} - \frac{\Delta^2}{2\omega} - \frac{q_2^2}{2\omega}\right]\right)^{-1} +$$

$$+ \; 1 \leftrightarrow 2 \; + \; (1 \leftrightarrow 1) \; + \; (2 \leftrightarrow 2) \Big] \qquad (4.2)$$

Here, contrary to the double scattering, terms with the same index for the elementary scattering matrices are present.

To evaluate the binding correction, we use following Kolybasov and Kondratyuk [24], the Lippman-Schwinger equation for the deuteron vertex function

$$\int \psi(\xi)\, T_{NN}\left(\vec{\xi}+\vec{\eta}_{/2}, \vec{q}_2 - \vec{\eta}_{/2}\right) d^3\xi = (16\pi^3 m^2)\left(\epsilon + \frac{(\vec{q}_2-\vec{\eta})^2}{m}\right) \psi(\vec{q}_2-\vec{\eta}) \qquad (4.3)$$

Using this equation and neglecting *) the square parentheses in the propagators of (4.2), the binding correction becomes

$$\hat{T}_B = \frac{1}{4}\sqrt{\frac{M}{\pi^3}} \int \frac{d^3\eta}{2m\omega} \Big[\frac{4(\vec{q}_2-\vec{\eta})\left(\epsilon + \frac{(\vec{q}_2-\vec{\eta})^2}{m}\right) T_2(\eta)\, T_1(\vec{\Delta}-\vec{\eta})}{(\eta_{11} + i\delta)^2}$$

$$+ \; 1 \leftrightarrow 2 \; + \; (1 \leftrightarrow 1) \; + \; (2 \leftrightarrow 2) \Big] \qquad (4.4)$$

*) This is a common procedure at high energies, provided the recoiling nucleons are non-relativistic.

Expanding now the propagator in (4.1) we find, neglecting terms of the order $1/\omega$, that

$$\hat{T}_D + \hat{T}_B = -\frac{1}{4}\sqrt{\frac{M}{\pi^3}}\frac{1}{2m\omega}\int d^3\eta \left[\frac{4(\vec{q}_2-\vec{\eta})\,T_2(\vec{\eta})\,T_1(\vec{\Delta}-\vec{\eta})}{\eta_{11}+i\delta} + (1\leftrightarrow 2)\right]$$

$$-\frac{1}{4}\sqrt{\frac{M}{\pi^3}}\frac{1}{2m\omega}\int d^3\eta \left[\frac{4(\vec{q}_2-\vec{\eta})\,T_2(\vec{\eta})\,T_1(\vec{\Delta}-\vec{\eta})\,(q_2^2-(\vec{q}_2-\vec{\eta})^2)}{2m\,(\eta_{11}+i\delta)^2}\right.$$

$$\left. + 1\leftrightarrow 2 + (1\leftrightarrow 1) + (2\leftrightarrow 2)\right] \qquad (4.5)$$

That means there is partial <u>cancellation between the dominant part of the binding correction and the recoil correction of the double scattering</u>. On the other hand, as shown above, the double scattering contributes very little to the high momentum tail of the "spectator" distribution: therefore even the binding correction is negligible in the same kinematical region.

Higher order multiple scattering terms such as triple scattering of Fig. 15c need not be calculated at high energies, since their sum is known to cancel the off-shell part of the double scattering term [25),26)].

4.3 <u>Final state interaction</u>

The diagram of Fig. 15d was already calculated in several references [27)] in two different limits: <u>at small momentum transfers</u> between a and c where the recoiling nucleons are non-relativistic and the nucleon-nucleon amplitude can be parametrized with the partial wave expansion [28)]; <u>at large momentum transfers</u> where the recoiling nucleon propagator can be linearized. The most reliable result is the one obtained in Ref. 27) at large momentum transfers: the reason is that for high momenta of the recoil we expect the off-shell effects to be small, while at low recoil energies these can be very large and model-dependent. From the result of Ref. 27) at large momentum transfers, it is tempting to conclude that the effect of final state interaction is small for high momenta of the spectators. This is confirmed by the application of the theory of Ref. 27) to the fine structure data, observed in the case of $K^+D \to K^{0*}pp$ (Fig. 8). Using the channel dependence we can actually conclude that this effect cannot be the common reason of the high momentum excess for the considered process. It is clearly shown in

Ref. 27) that the effect on the spectator distribution consists of a slight suppression of the low momentum part and an enhancement of the high momentum part: the prediction R_f for the quantity f in this model is found to be (see Fig. 15)

$$R_f = \frac{\sigma(a\to c)\, A}{\sigma(a\to c) - \sqrt{\sigma(a\to c)}\, B} \tag{4.6}$$

where A and B are channel-independent quantities. Expanding we find:

$$R_f \sim A\left(1 + \frac{B}{\sqrt{\sigma(a\to c)}}\right) \tag{4.7}$$

While the dominant term is channel-independent, the correction depends on the channel, but it is of the order of a few percent which cannot account for the fluctuations in f of the order of 100% found experimentally (Fig. 5).

4.4 t exchange

Another interesting proposal was put forward by Poster and Schlein [14], who considered the forward peak in the t distribution of Fig. 8 as evidence for a π exchange to the entire deuteron. This mechanism is represented in Fig. 16a: while the upper vertex is related to the decay of K^{o*}, the lower one is calculated using the data for pion absorption by deuteron. In this model, the prediction R_f for f can be represented graphically by

$$R_f \sim \frac{\int \left| \right|^2 d^3p}{\int \left| \right|^2 d^3p} \tag{4.8}$$

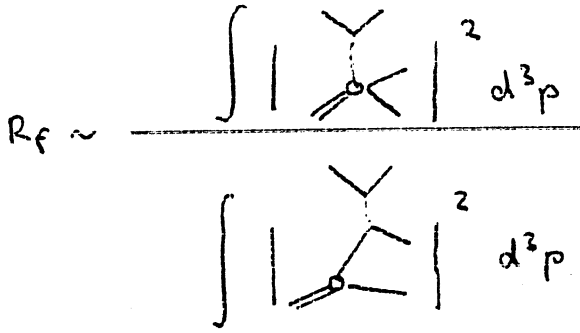

Note that in the denominator, the total yield is approximated by the spectator model. This approximation does not change our reasoning: if the numerator is summed incoherently to the spectator model, then R_f is a power series of the above ratio; the interference term is a small effect which we can neglect as in the previous case.

From (4.8) it is clear that R_f is independent of the upper vertex, and we expect equal f for ρ^o and K^{o*} production: we know, however, that this prediction of the model is not verified. One can overcome this difficulty, assuming that for the deuteron (numerator) the ρ exchange is important for K^{o*} production, while for the nucleon (denominator) the π exchange is known to be dominant in both cases. This reasoning is, however, impractical because of phase problems, and we prefer to use for the phenomenological analysis another model.

4.5 Meson exchange

Several people [29] in the 1950's found the idea of meson exchange useful to explain singular effects in photo-disintegration of the deuteron at high energies. The interest of this idea is still alive in more recent work by Delorme, Ericson and Fäldt [30] and in a series of papers concerned with weak and electromagnetic interactions with nuclei [31]. In this series of papers, one deals essentially with two types of diagrams which we draw for the case we are interested in (Fig. 16b, c).

The meson exchange diagram of Fig. 16b has been calculated for inelastic electron scattering on deuteron at low energies [31] and found to give a small contribution, whereas the diagram of Fig. 16c was found to be important. The following simple considerations, based on the channel dependence, lead essentially to the same conclusions. Let us consider, for instance, the values of f for $\pi^+ \to \pi^o$ and for $\pi^+ \to \rho^o$: both production amplitudes are dominated by one Regge pole, the ρ pole in the first case and the pion pole in the second. However, while for the first case the same exchange is possible in diagram 16b, for the second the π exchange is forbidden on account of G parity conservation at the lower vertex. Any other exchange is forbidden for the same reason, i.e., equivalent to a strong suppression of the predicted value for f in the second case. On the other hand, the experimental values of f are of the same order and therefore cannot be explained by this mechanism.

To evaluate the qualitative prediction of the diagram 16c, we simply calculate the relative rate of production of one additional pion

$$R_\pi = \frac{\sigma(aN \to cN\pi)}{\sigma(aN \to cN)} \qquad (4.9)$$

and we compare it to f. This procedure is equivalent to assuming that the contribution of the meson exchange effect is

$$\sigma_{ME} = \sigma(aN \to cN\pi) \cdot P_\pi \qquad (4.10)$$

where P_π is the probability of re-absorption of the additional pion *). This simple phenomenological treatment allows a qualitative comparison with the values of f for different processes. Since the pion is virtual, its charge is not defined; therefore in (4.11) the numerator is the coherent sum of two terms, corresponding to different charges of the pion. For instance, for the reaction $K^+D \to K^{o*}pp$ one should sum coherently the contribution of the reactions $K^+p \to K^{o*}\pi^+p$ and $K^+n \to K^{o*}\pi^o p$. While the total rate for the first reaction can be found in the data compilation [33),34)], the rate for the second reaction is not known experimentally, as in many other cases where at least two neutrals are involved. But we can consider, at least in a first approximation, only the first term: it is unlikely that the addition of the second term changes the channel dependence drastically. The results of the comparison are shown in Fig. 17 where R_π is already multiplied by P_π and assumed to be 20%. The figure shows the over-all features of the channel dependence are reproduced and provide a strong indication that the idea of meson exchange is correct.

In order to include the π^o term we assume that the additional pion is the decay product of a Δ resonance produced via a Regge exchange (Fig. 18). This assumption is reasonable, close to the production threshold, and provides a method for selecting only slow pions which are the only natural candidates for re-absorption. In this model one can calculate the π^o production rate from the known rate, using Clebsch-Gordan coefficients. This procedure has been checked in one case, where the π^o rate is experimentally known, finding reasonable agreement. On the other hand the πNN vertex has a Clebsch-Gordan coefficient different from the π^+ case and a phase factor enters from the exchange symmetry in the deuteron vertex: hereby we can simply substitute $(\sqrt{\sigma_+} + \sqrt{\sigma_o/2})^2$ instead of σ_{π^+} in (4.12). Using this prescription and the analogous one for π^-, we obtain values for f indicated as double circles in Fig. 17. The results show a qualitative agreement with experiment, as was already seen without considering the π^o exchange. In some cases such as the $\pi^+ \to \pi^o$ series, the agreement is even quantitative. Furthermore, the parameter is pulled down to 15%.

However, for incident K^- this model does not seem to be valid because for the $\Sigma\pi$ channels the value of P_π is abnormally high: $P_\pi \gtrsim 1$.

---

*) R. Wilson [32)] gives a phenomenological description of the same type for the photo-distintegration of the deuteron which fits the integrated rate around 300 MeV surprisingly well.

4.6 Isobars in the final scattering state

A way out of the above difficulty is to assume that the recoiling baryon inside the triangular diagram 15d can be different from the external one. For the hyperon case this would mean that while for the $\Sigma^-\pi^+$ case, only the elastic scattering $\Sigma^-n \to \Sigma^-n$ is possible, whereas for $\Sigma^+\pi^-$ one should consider in the final state interaction also $\Lambda p \to \Sigma^+n$. This last process is related by isospin invariance and time reversal to the known one $\Sigma^-p \to \Lambda n$. Recalling [35),36)] that the cross-section for this last process is quite large and comparable with the elastic cross-section $\Sigma^+n \to \Sigma^+n$, we understand qualitatively the different values of f for the last two cases of Fig. 17. On the other hand, the $\Lambda\pi^-$ case is perfectly equivalent to the previous one as far as the final state interaction is concerned, but the cross-section $\sigma(K^-n \to \pi^-\Lambda)$ is twice the cross-section $\sigma(K^-p \to \pi^-\Sigma^+)$ and this explains qualitatively the difference between the f's. This interpretation of the high momentum components in the hyperon case is in agreement with a recent theoretical work [37)] done to explain the peaks in the Λp invariant mass in the last case.

For the two-nucleon case, the natural isobar is the Δ resonance. Therefore the previous analysis is still valid provided we call P_π the probability for the process $\Delta N \to NN$ to occur. From this point of view since the cross-section for $pp \to \Delta^{++}n$ [33)] is of the same order as the pp elastic cross-section at threshold, the importance of the Δ isobar component is clear, at least in the kinematical region of the threshold. Actually, similar peaks to the Λp case in the invariant mass of the two nucleons are being seen in pD experiments *).

5. CONCLUSIONS

From the discussion of the channel dependence, in the two-nucleon case, it seems to be plausible that the cause of the high momentum excess is a meson exchange effect. However, to understand the hyperon data, we have to introduce isobars in the final state interaction. This picture is equivalent to the meson exchange, because in the reaction $NN \to \Delta N$ pi-meson exchange plays the important rôle being the Born term.

---

*) Private communication by J. Stepaniak and T. Siemiarczuk of the Dubna-Warsaw Collaboration. The above hypothesis was formulated by this collaboration [13)] for the first time.

If this interpretation is confirmed by more theoretical studies, one should investigate the consequences in other processes like:

1) $\bar{p}D$ annihilation at low energies, where both $\bar{p}$ and $\bar{\Delta}$ should be produced virtually in triangular diagrams, considered by the Shapiro group [38] and could simulate resonances in the $\bar{p}n$ invariant mass [39], exactly in the same way as on the Λp invariant mass in the reaction $K^-D \to \Lambda\pi^-p$;

2) deep inelastic electron scattering on deuteron where the extracted neutron inelastic form factor could change for large values of the Feynman variable x [2] ;

3) knock out reactions on nuclei like $(p,2p)$ and $(e,e'p)$, for high momenta of the nuclear recoil, where the Δ components should be taken into account in the final state interaction [40].

ACKNOWLEDGEMENTS

The authors have profited of many discussions with the colleagues in the Theoretical Study Division at CERN, especially with T. and M. Ericson, M. Rho, C. Wilkin, G. Fäldt and F. Schrempp. One of us (G.A.) is grateful also to M. Ferro-Luzzi for encouragement, to E. Castelli for a lot of help in computer drawing, and R. Odorico for discussions on Regge poles. We thank also P. Zielinski for providing us with the unpublished data for f in the proton case.

APPENDIX A

To calculate the cross-sections (2.4) and (2.6), we use the closure sum rule

$$\frac{d\sigma}{dt} = \frac{1}{3} \sum_i \langle i | \Omega^+ \Omega | i \rangle = \langle \Omega^+ \Omega \rangle \tag{A.1}$$

where i are the spin states of the deuteron and Ω is the scattering operator

$$\Omega = \text{const} \times \langle I_f | \hat{O}_{12} | I_i \rangle \tag{A.2}$$

Calling $\hat{S}(q_i)$ the tensor operator, the basic sum rules are

$$\begin{aligned}
&\langle \hat{S}(q_i) \rangle = \langle \vec{H} \cdot \vec{\sigma}_j \, \hat{S}(q_i) \rangle = 0 \\
&\langle \hat{S}^2(q_i) \rangle = 1 \\
&\langle (\vec{H} \cdot \vec{\sigma}_i)(\vec{G} \cdot \vec{\sigma}_j) \rangle = \frac{1}{3} (1 + 2\delta_{ij}) \, \vec{H} \cdot \vec{G} \\
&\langle (\vec{H} \cdot \vec{\sigma}_i)(\vec{G} \cdot \sigma_j) \hat{S}(q_\ell) \rangle = (1 - \delta_{ij}) \sqrt{2} \times \\
&\qquad \times \left[(\vec{G} \cdot \hat{q}_\ell)(\vec{H} \cdot \hat{q}_\ell) - \frac{1}{3} \vec{H} \cdot \vec{G} \right]
\end{aligned} \tag{A.3}$$

Using these sum rules one can derive other ones

$$\begin{aligned}
&\langle \hat{S}(q_1) \, \hat{S}(q_2) \rangle = \frac{1}{2} \left(3 (\hat{q}_1 \cdot \hat{q}_2)^2 - 1 \right) \\
&\langle (\vec{H} \cdot \vec{\sigma}_1)(\vec{G} \cdot \vec{\sigma}_2) \hat{S}(q_1) \, \hat{S}(q_2) \rangle = \frac{2}{3} \vec{G} \cdot \vec{H} \\
&- \frac{1}{2} \left[(\vec{G} \cdot \hat{q}_1)(\vec{H} \cdot \hat{q}_2) + (\vec{G} \cdot \hat{q}_2)(\vec{H} \cdot \hat{q}_1) \right] \\
&- \frac{3}{2} \left[\vec{G} \cdot (\hat{q}_1 \times \hat{q}_2) \right] \left[\vec{H} \cdot (\hat{q}_1 \times \hat{q}_2) \right]
\end{aligned} \tag{A.4}$$

$$\langle \vec{H} \cdot \vec{\sigma}_i \, \hat{S}(q_1) \, \hat{S}(q_2) \rangle = \frac{3}{2} \, i \, (\hat{q}_1 \cdot \hat{q}_2) \, \vec{H} \cdot (\hat{q}_1 \times \hat{q}_2)$$

APPENDIX B

The double scattering diagram in the case of elastic scattering (Fig. 19a) can be written down using the rules of Ref. 5)

$$\hat{T}_D = \frac{1}{16\pi^3} \int \frac{d^3p\, d^3q}{2\omega m} \psi(\vec{p})\, \psi\left(\vec{p}+\vec{q}-\frac{\vec{\Delta}}{2}\right) \sum_{i\neq j} \frac{T_i(\vec{q})\, T_j(\vec{\Delta}-\vec{q})}{q_z - \alpha + i\delta}$$

$$= -\int d^3p\, d^3q\, \Psi(\vec{p},\vec{q}\,|\,\vec{\Delta})\, \frac{1}{q_z - \alpha + i\delta} \qquad (B.1)$$

with the same notation of Eq. (4.1) ; α is the correction to the eikonal propagator due to the nucleon recoil and the transverse part of the momentum transfer

$$\alpha = \frac{1}{2k}\left[q^2 + 2\omega\left(\epsilon + \frac{p^2}{2m} + \frac{(\vec{p}+\vec{q})^2}{2m}\right)\right] \qquad (B.2)$$

Using the same prescription of Bertocchi and Capella [41] reformulated in a systematic way in Ref. 5) to calculate a Feynman graph, we find, for the binding diagram (Fig. 19b)

$$\hat{T}_B = \frac{1}{2(2\pi)^5 m^2} \int \frac{d^3p_1\, d^3p_2\, d^3q}{2m\omega}\, \psi(p_1)\, \psi\left(\vec{p}_2 - \frac{\vec{\Delta}}{2}\right) \times$$

$$\times \sum_{i,j=1}^{2} \frac{T_i(\vec{q})\, T_j(\vec{\Delta}-\vec{q})\, T_{12}\left(\vec{p}_1 - (-1)^{i+j}\,\vec{q}/2,\ \vec{p}_2 + \vec{q}/2\right)}{\left[q_z - \epsilon - \frac{(\vec{p}_1+\vec{q}/2)^2}{m} - \frac{q^2}{4m} + i\delta\right]\left[q_z - \epsilon - \frac{(\vec{p}_2-\vec{q}/2)^2}{m} - \frac{q^2}{4m} + i\delta\right]} \qquad (B.3)$$

Using the identity (4.3) we find

$$\hat{T}_B \sim \int d^3p\, d^3q\, \Psi(\vec{p},\vec{q}\,|\,\vec{\Delta})\ \frac{(\epsilon + p^2/m)}{(q_z + i\delta)^2} +$$

$$+ \sum_i \int d^3p\, d^3q\ \frac{T_i(\vec{q})\, T_i(\vec{\Delta}-\vec{q})\, \psi(p)\, \psi(\vec{p} - \frac{\vec{\Delta}}{2})\, (\epsilon + p^2/m)}{(q_z + i\delta)^2} \qquad (B.4)$$

Expanding the propagator in (B.1)

$$\frac{1}{q_z - \alpha + i\delta} \sim \frac{1}{q_z + i\delta} + \frac{\alpha}{(q_z + i\delta)^2} \qquad (B.5)$$

we obtain the result that in neglecting the first term of α, which vanishes at high energy as $1/\kappa$, there is a cancellation between (B.1) and the first term of (B.3) : the remainder is

$$\hat{T}_D + \hat{T}_B = \hat{T}_D^{eik} + \int d^3p\, d^3q\, \Psi(\vec{p},\vec{q}\,|\,\vec{\Delta})\ \frac{\left(\frac{p^2}{2m} - \frac{(\vec{p}+\vec{q})^2}{2m}\right)}{(q_z + i\delta)^2} +$$

$$+ \sum_i \frac{i}{8\pi^2} \int \frac{d^3p\, d^3q}{2m\omega}\ \frac{T_i(\vec{q})\, T_i(\vec{\Delta}-\vec{q})\, \psi(p)\, \psi(\vec{p} - \vec{\Delta}/2)}{(q_z + i\delta)^2}\ (\epsilon + p^2/m)$$

The second term can be shown to be exactly zero in the forward direction ; the third one should be cancelled in the same way by the off-shell corrections to the single scattering, as shown recently by Fäldt [42] in another context : unfortunately to show this cancellation one needs a complete dynamical theory, like for instance the multiperipheral model [43] which is beyond the scope of the present work.

REFERENCES

1) C.F. Perdrisat et al. - Phys.Rev. 187, 1201 (1969) ;
D.C. Brunt, M.J. Clayton and B.A. Westwood - Phys.Rev. 187, 1856 (1969).

2) G. West - Phys.Letters 37B, 509 (1971).

3) R.V. Reid - Ann.Phys.(N.Y.) 50, 911 (1968).

4) D.W.L. Sprung - Invited talk given at Quebec Conference on Four-Body Problems (August 1974).

5) G. Alberi, E. Castelli, P. Poropat and M. Sessa - INFN-AE 72/3 (1972).

6) G. Alberi - INFN-AE 73/1 (1973).
G. Alberi and L.P. Rosa - Nuclear Phys. B83, 218 (1974).

7) E. Byckling and K. Kajantie - "Particle Kinematics", S. Wiley and Sons (1973).

8) A.K.M.A. Islam - Ph.D. Thesis, Rutherford Lab., Internal Report, HEP/T/39

9) G. Giacomelli et al. (B.G.R.T. Collaboration) - Nuclear Phys. B37, 577 (1972).

10) G.C. Benson - Ph.D. Thesis (1968), University of Michigan, unpublished.

11) B. Musgrave - in Proceedings of the Conference on the Phenomenology of Particle Physics, California Institute of Technology, Pasadena, CA (March 1971).

12) K. Buchner et al. - Nuclear Phys. B45, 333 (1972) ;
G. Dehm et al. - Nuclear Phys. B60, 493 (1973).

13) B.S. Aladashvili et al. - Nuclear Phys. B86, 461 (1975).

14) R. Poster et al. - Phys.Rev.Letters 33, 1625 (1974).

15) P. Benz et al. - in Proceedings of 1971 International Symposium on Electron and Photon Interactions at High Energies, Ithaca, p. 338 ; and Nuclear Phys. B65, 158 (1973) ;
D.H. White, R.M. Schechtan and B.M. Chasan - Phys.Rev. 120, 614 (1960).

16) B.Y. Oh et al. - Nuclear Phys. B51, 57 (1973) ;
P.S. Eastman et al. - Ibid. 29 (1973).

17) R.K. Rader et al. - Phys.Rev. D6, 3059 (1972).

18) CERN-Heidelberg-Munich Collaboration, paper in preparation ;
V. Hepp - "$\bar{K}n$ Cross-Sections between 1600 and 1750 MeV", CERN/D.Ph.II/Divers (23 June 1975).

19) N.W. Dean - Phys.Rev.Letters 27, 276 (1971).

20) R.J. Glauber and V. Franco - Phys.Rev. 156, 1685 (1967) ;
L. Bertocchi - Nuovo Cimento 50A, 1015 (1967).

21) G. Alberi, L.P. Rosa and Z.D. Thomé - Phys.Rev.Letters 34, 503 (1975).

22) J.V. Allaby et al. - Phys.Letters 30B, 549 (1969) ;
R.J. Glauber, O. Kofoed-Hansen and B. Margolis - Nuclear Phys. B30, 220 (1971).

23) D.I. Julius - Ann.Phys.(N.Y.) 87, 17 (1974).

24) V.M. Kolybasov and L.A. Kondratyuk - Phys.Letters 39B, 439 (1972).

25) D.R. Harrington - Phys.Rev. 184, 1745 (1969).

26) J.M. Eisenberg - Ann.Phys.(N.Y.) 71, 542 (1972).

27) C. Smith and C. Wilkin - Ann.Phys.(N.Y.) 75, 103 (1973) ;
G. Alberi, M.A. Gregorio and Z.D. Thomé - Nuovo Cimento 19A, 585 (1974).

28) M.H. McGregor, R.A. Arndt and R.M. Wright - Phys.Rev. 169, 1149 (1968).

29) L.D. Pearlstein and A. Klein - Phys.Rev. 118, 193 (1960), and references therein.

30) J. Delorme, M. Ericson and G. Fäldt - Nuclear Phys. A240, 493 (1975).

31) E. Hadjimichael - Talk given at the Conference on Mesonic Effects in Nuclei, Saclay (May 1975), IPNO/TH 75-21 and references therein, in particular : J. Hockert, D.D. Riska, M. Gari and A. Huffmann - Nuclear Phys. A217, 14 (1973).

32) R. Wilson - Phys.Rev. 104, 218 (1956).

33) E. Bracci et al. - CERN/HERA 72-1 ($\pi^{\pm}$), 72-2 ($K^{\pm}$), 73-1 ($p-\bar{p}$).

34) D. Lüke and P. Söding - Springer Tracts in Modern Physics 59, 39 (1971).

35) R. Engelmann, H. Filthuth, V. Hepp and E. Kluge - Phys. Letters 21, 587 (1966);
F. Eisele, H. Filthuth, W. Föhlisch, V. Hepp, E. Leitner and G. Zech, Phys. Letters 37B, 204 (1971).

36) G. Alexander and U. Karshon - in High Energy Physics and Nuclear Structure, Rehovoth (1967).

37) T. Ishihara, Y. Iwamura, Y. Takahashi and E. Satoh - in Abstracts of Contributed Papers, VI International Conference on High Energy Physics and Nuclear Structure,

38) O.D. Dalkarov - in Proceedings of the Seminar on "Interactions of High Energy Particles with Nuclei and New Nuclear-Like Systems", Moscow, ITEP (September 1973).

39) T.E. Kalogeropoulos and G.S. Tzanakos - Phys.Rev.Letters 34, 1047 (1975).

40) U. Amaldi - in "Few Particle Problems in the Nuclear Interaction", Los Angeles (1972) ;
D.F. Jackson - in International Conference on Nuclear Structure and Spectroscopy, Amsterdam (1974).

41) L. Bertocchi and A. Capella - Nuovo Cimento 51A, 369 (1967).

42) G. Fäldt - Lund Preprint LU-TP-74/13.

43) D. Amati, A. Stanghellini and S. Fubini - Nuovo Cimento 26, 6 (1962).

44) D. Merril et al. - Nuclear Phys. B18, 403 (1970).

FIGURE CAPTIONS

Figure 1 The kinematics of the two nucleons before (left) and after (right) the interaction with the incident particle.
a) for small scattering angles for the incident particle, such that Δ is comparable with q_1 ;
b) for large scattering angles.

Figure 2 a) Predicted spectator distribution, according to the impulse approximation, including the misidentification effect, for the process $K^+D \to K^{0*}pp$ at 2 GeV/c (solid line). The dashed line is the result without the misidentification terms (2.14). The open circles are the result of (2.13). The crosses correspond to the probability function (2.12). The wave function is taken from Reid [3] (soft core).
b) The same as for a) for the process $K^+D \to K^{*+}n\ (p_s)$ at 1.4 GeV/c (solid curve). The dashed curve is the same as for a).

Figure 3 The fraction f of events with spectator protons of momentum greater than 250 MeV/c for reactions of the type $\pi^+D \to X^0pp$. The particles X^0 are listed below the experimental points [10].

Figure 4 The fraction f as function of the number of pions [10].

Figure 5 The parameter f for different processes.
: Ref. 9) ; : Ref. 12) ; : Ref. 10) ; : Ref. 13) ; : Ref. 16) ; : Ref. 1), the left point being at 1.825 GeV/c and the right one at 2.110 GeV/c ; : Ref. 15) I) ; : Ref. 15) II), the first point from 230 to 500 MeV photon energy, the second from 500 to 1000 MeV.

Figure 6 f for nine channels in the interaction K^-D at 700-850 MeV/c [18]. For the first two channels corresponds to the energy average, and corresponds to 750 and 850 MeV/c, respectively.

Figure 7 f as a function of Δ^2 for ρ^0 and f^0 production.

Figure 8 The differential cross-section, for the reaction $K^+D \to K^{o*}pp$ at 2 GeV/c, selecting the invariant mass of the two protons between 2.13 and 2.19 GeV. The experimental data are from Ref. 14). The solid line is the prediction of the impulse approximation and the dashed line is obtained by adding coherently the final state interaction diagram (Fig. 15d).

Figure 9 The spectator distribution for the reaction of $Dp \to ppn$ at 3.3 GeV/c for the deuteron, equivalent to 1.66 GeV/c for the proton [Ref 13]. The dotted line is the probability $\mathcal{P}$ (p) for the Reid wave function (hard core), normalized to the experimental data in the integral from 0 to 250 MeV/c.

Figure 10 The same as Fig. 9 for the reaction $\gamma D \to \pi^- pp$ from 0.2 to 2 GeV/c [Ref. 15) I].

Figure 11 Comparison between different spectator distributions : ⧫ : $\bar{p}D \to K\bar{K}\pi$'s(p_s) at 1.09 + 3.45 GeV/c [Ref. 16)] ; ⧈ : $\pi^+D \to 4\pi pp$ at 1.1 + 2.4 GeV/c [Ref. 17)] ; ✱ for $K^+D \to K^+\pi^-pp$ at 4.6 GeV/c [Ref. 12, I]. The solid and dashed lines correspond, respectively, to the hard and soft core versions of the Reid wave function.

Figure 12 Same as for Figs. 9 and 10, for the reaction $K^+D \to K^o pp$ [Ref. 9].

Figure 13 Comparison between annihilation data of Fig. 11 and the reaction $KD \to (\Lambda \text{ or } \Sigma)\pi$'s (n_s)) (✱) at 3 GeV/c [Ref. 44].

Figure 14 Comparison between annihilation data [16] and the reaction $K^-D \to \Sigma^+\pi^- n_s$ at 700 + 850 MeV/c [18] (O : the statistical error is inside the circle).

Figure 15 Multiple scattering diagrams :

a) double scattering ;

b) binding effect ;

c) triple scattering ;

d) final state interaction.

Figure 16 Meson exchange diagrams.

Figure 17 Comparison of f with the prediction of the phenomenological model (4.12) : 0 is the result, if only one charged pion is exchanged, and ⊙ if one adds coherently the contribution of the π^0, $P_\pi = 20\%$ and 15%, respectively. For the last two channels ($\Sigma\pi$) $P_\pi = 1$.

Figure 18 Diagram for Δ production in the final state via Regge exchange.

Figure 19 a) double scattering diagram;
b) binding diagram.

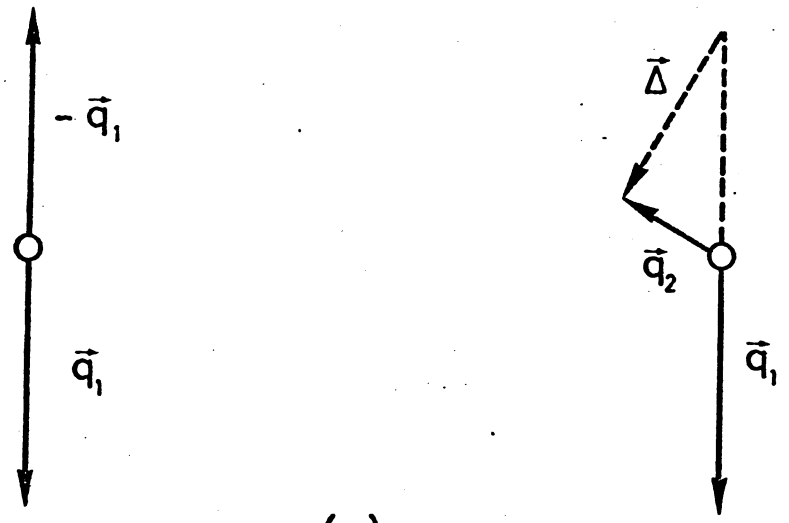
$-\vec{q}_1$
$\vec{q}_1$
$\vec{\Delta}$
$\vec{q}_2$
$\vec{q}_1$

(a)

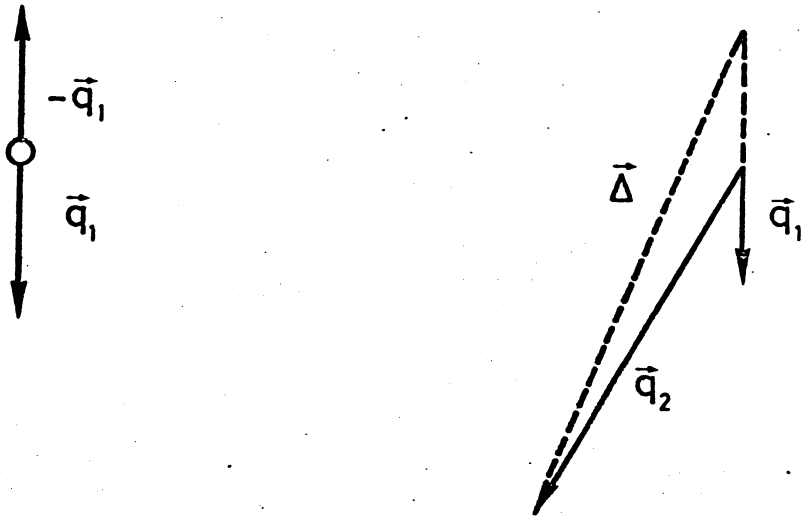
$-\vec{q}_1$
$\vec{q}_1$
$\vec{\Delta}$
$\vec{q}_1$
$\vec{q}_2$

(b)

FIG. 1

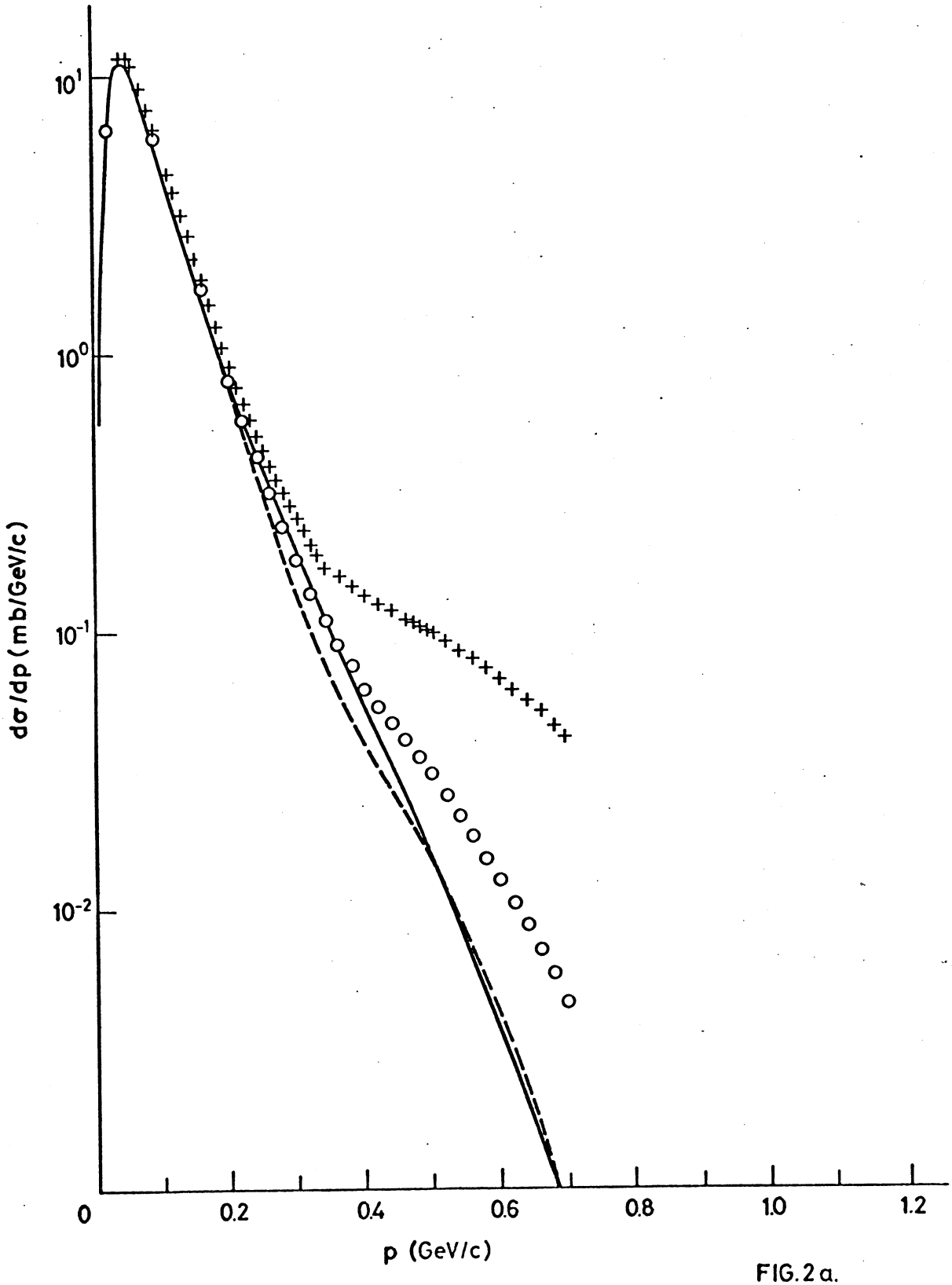

FIG. 2 a.

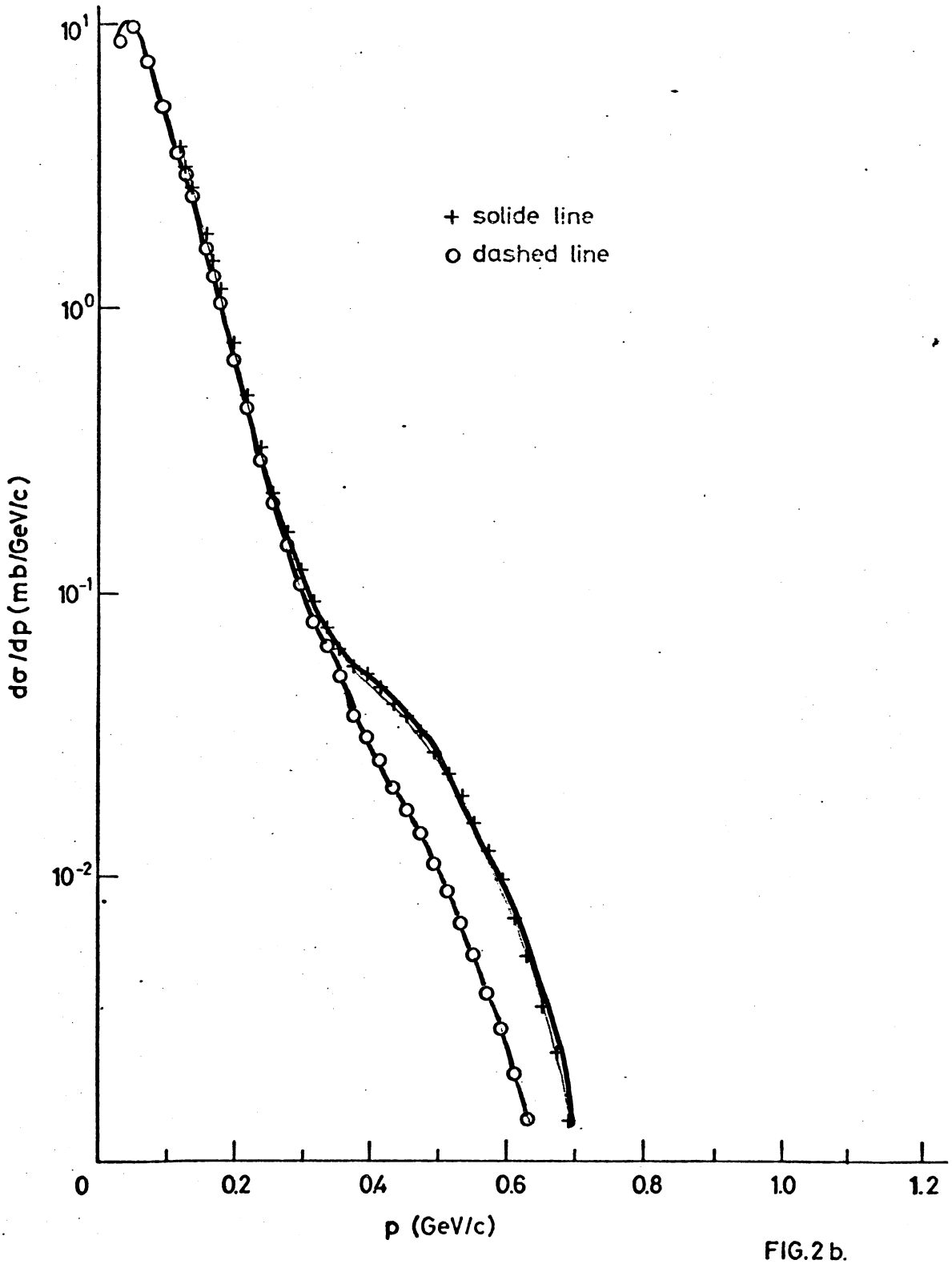
+ solide line
o dashed line
10^1
10^0
10^{-1}
10^{-2}
dσ/dp (mb/GeV/c)
0
0.2
0.4
0.6
0.8
1.0
1.2
p (GeV/c)

FIG. 2 b.

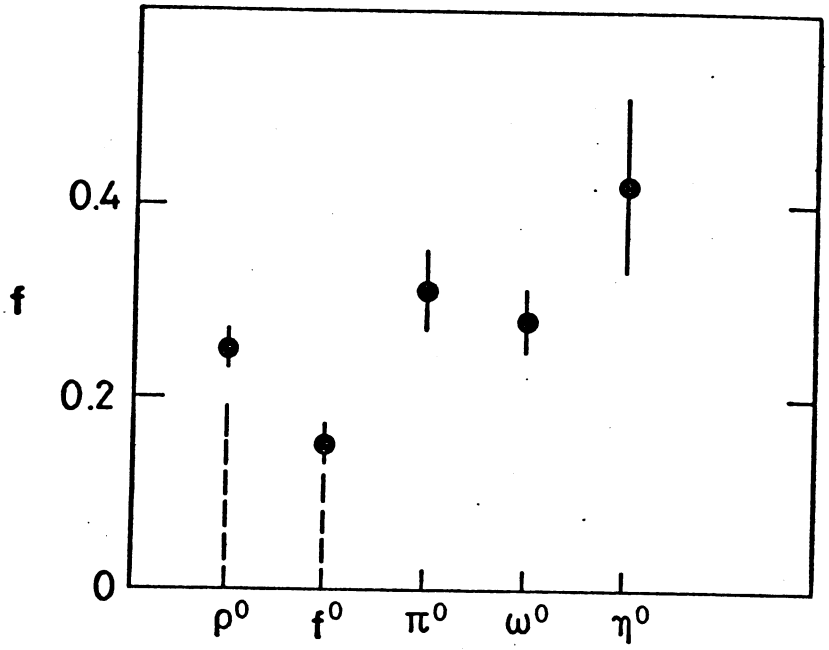

FIG. 3

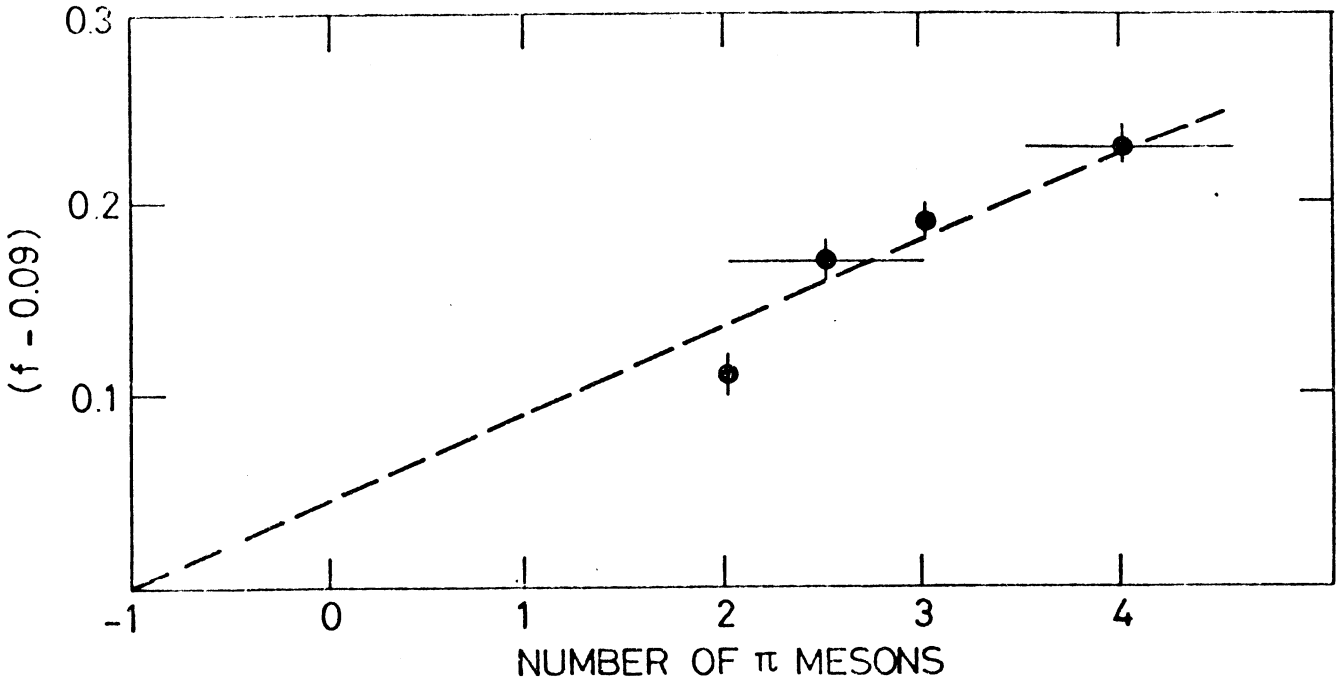

FIG. 4

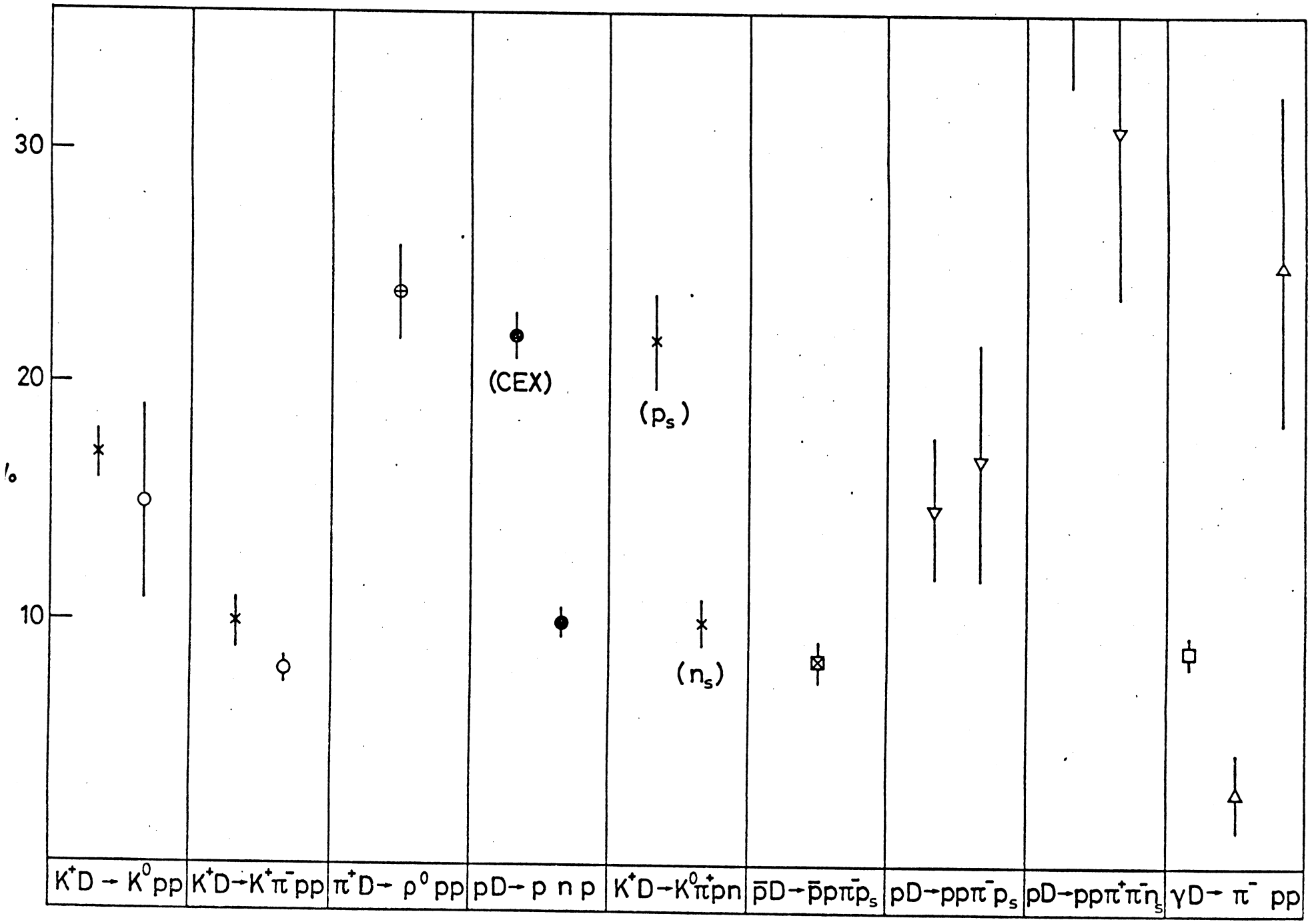
30
20
10
(CEX)
(p_s)
(n_s)
K⁺D → K⁰pp
K⁺D→K⁺π⁻pp
π⁺D→ ρ⁰pp
pD→ p n p
K⁺D→K⁰π⁺pn
p̄D→p̄pπ⁻p_s
pD→ppπ⁻p_s
pD→ppπ⁺π⁻η_s
γD→ π⁻ pp

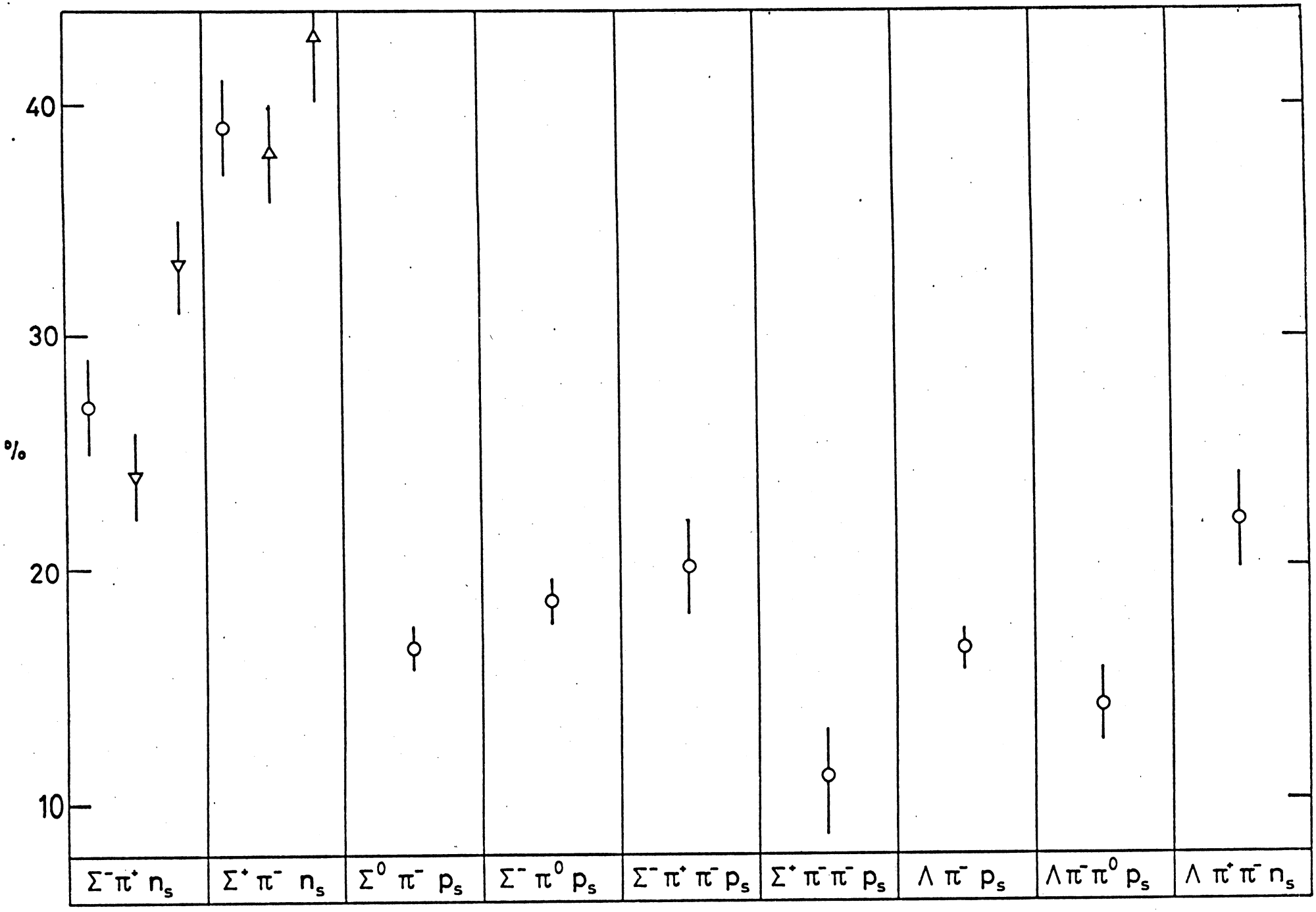
40
30
20
10
%
$\Sigma^- \pi^+ n_s$
$\Sigma^+ \pi^- n_s$
$\Sigma^0 \pi^- p_s$
$\Sigma^- \pi^0 p_s$
$\Sigma^- \pi^+ \pi^- p_s$
$\Sigma^+ \pi^- \pi^- p_s$
$\Lambda \pi^- p_s$
$\Lambda \pi^- \pi^0 p_s$
$\Lambda \pi^+ \pi^- n_s$

FIG. 6

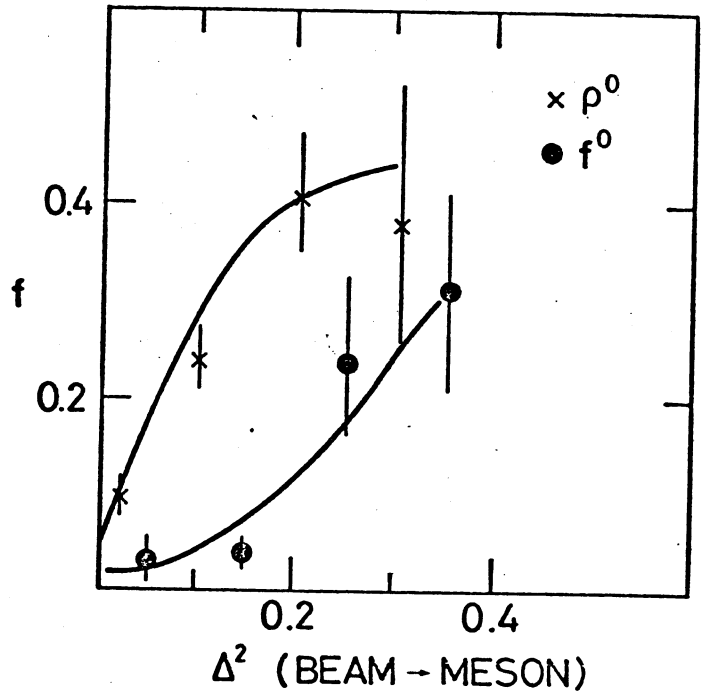

FIG. 7

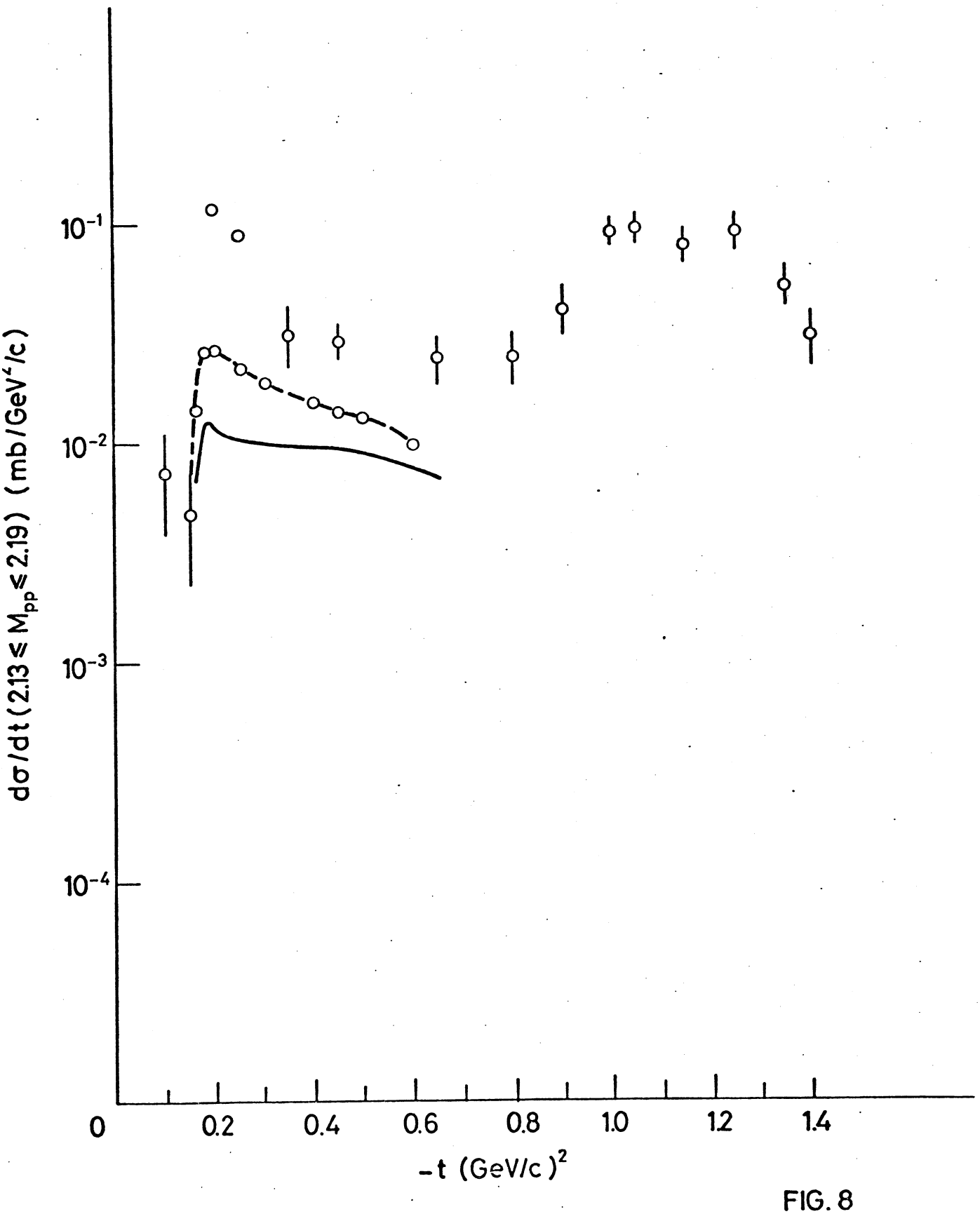
10^{-1}
10^{-2}
10^{-3}
10^{-4}
$d\sigma/dt\,(2.13 \leq M_{pp} \leq 2.19)$ (mb/GeV^4/c)
0
0.2
0.4
0.6
0.8
1.0
1.2
1.4
$-t$ (GeV/c)^2

FIG. 8

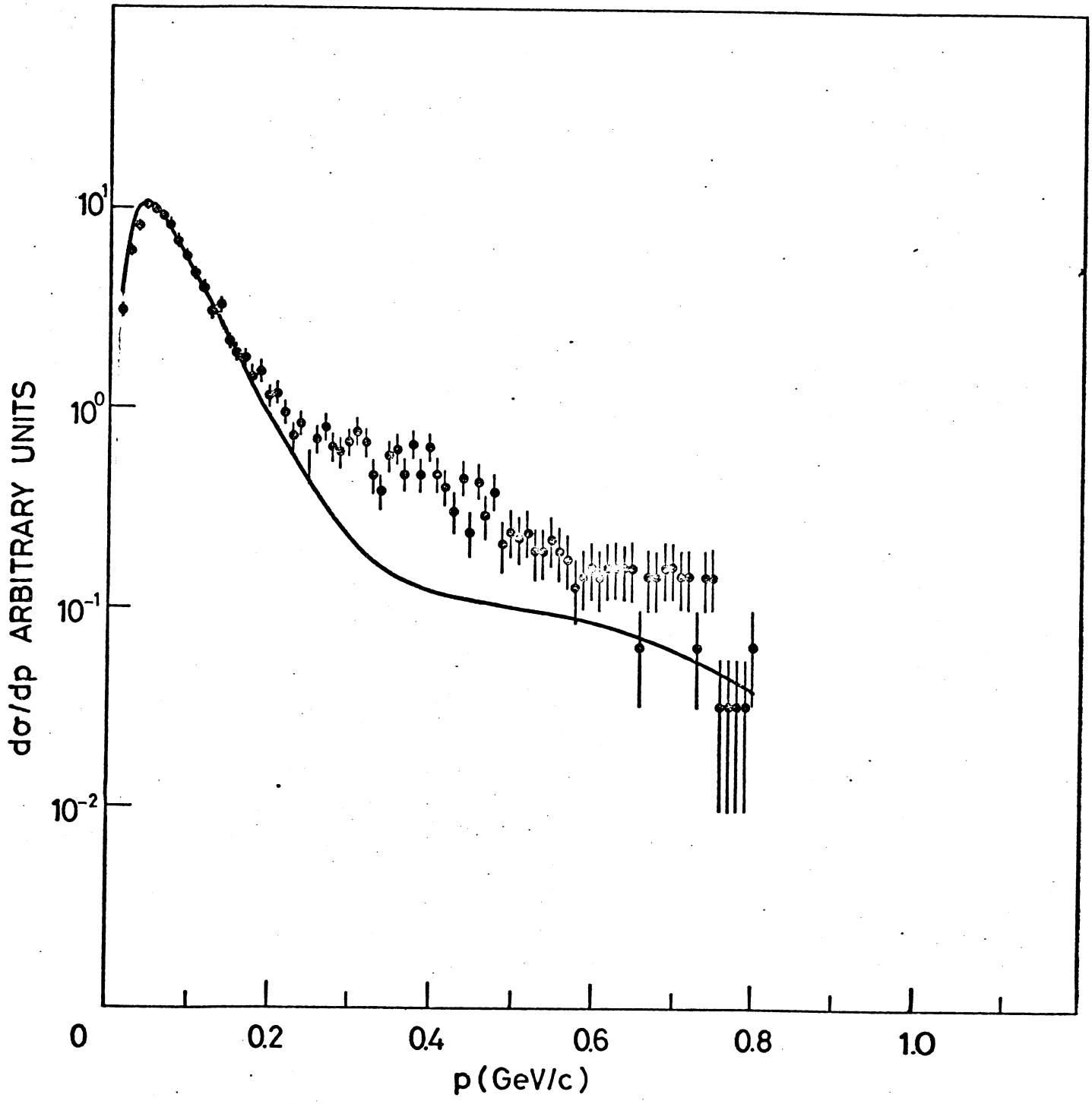

FIG. 9

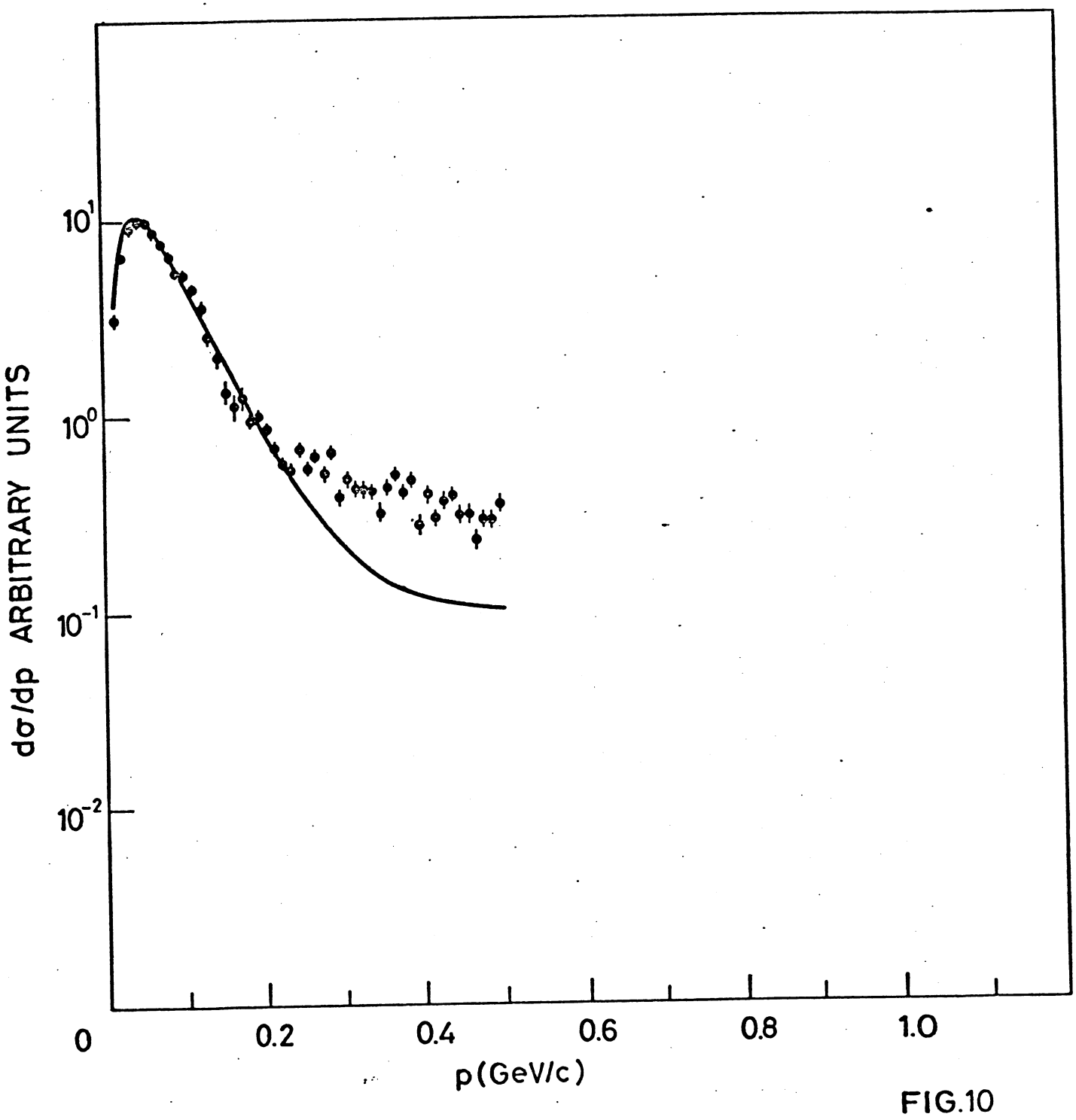

FIG.10

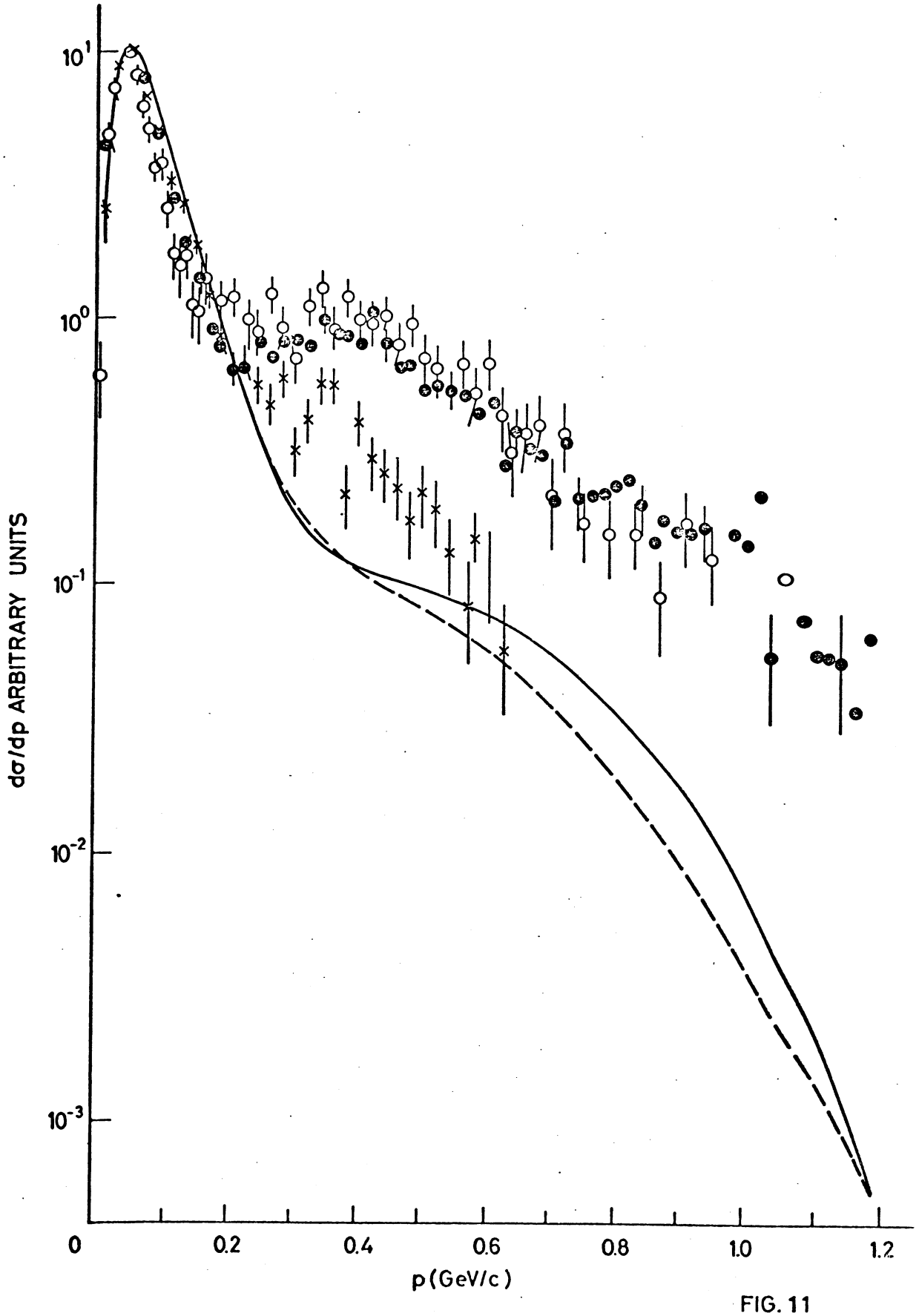
10^1
10^0
10^{-1}
10^{-2}
10^{-3}
dσ/dp ARBITRARY UNITS
0
0.2
0.4
0.6
0.8
1.0
1.2
p(GeV/c)

FIG. 11

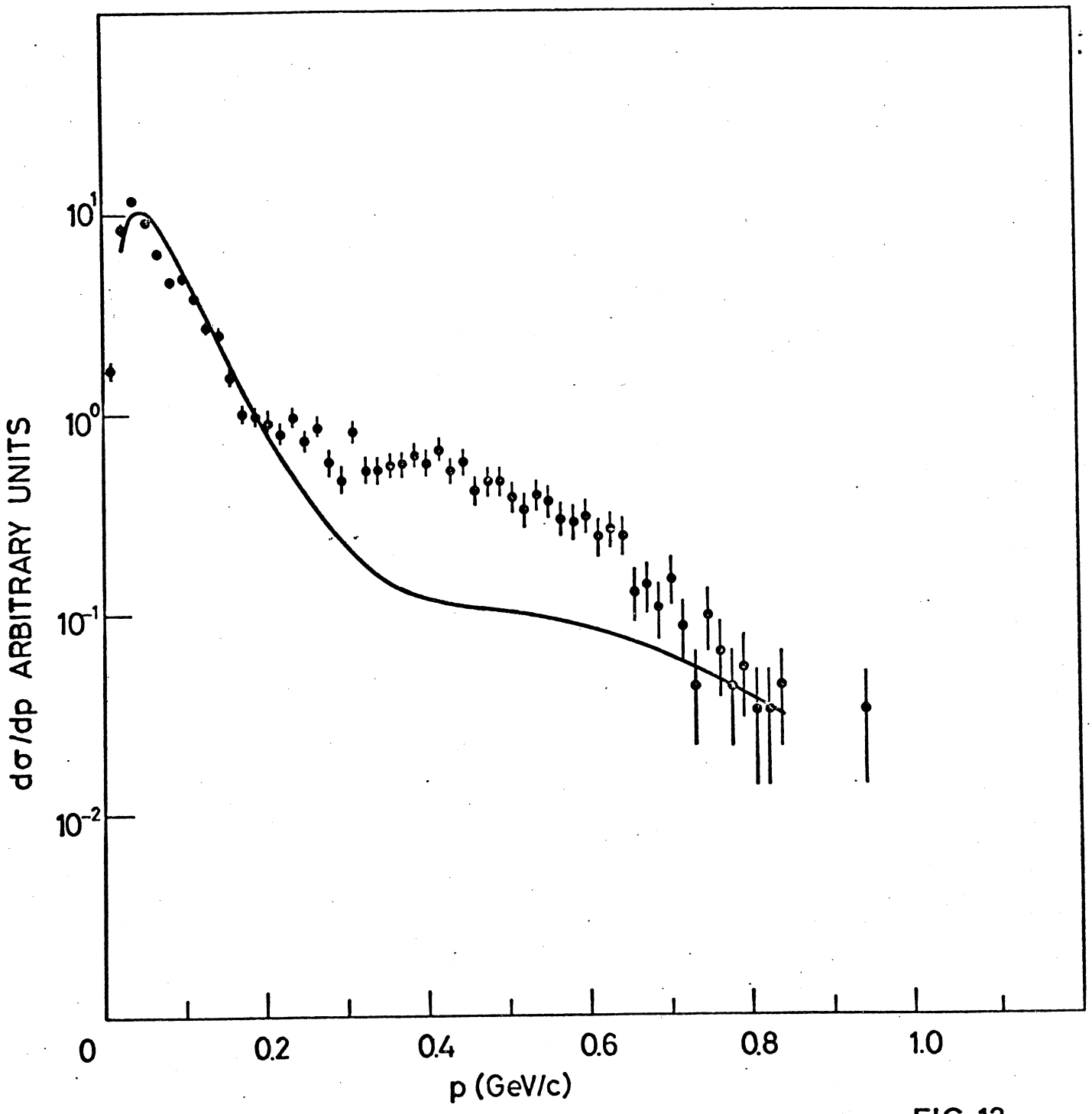

FIG. 12

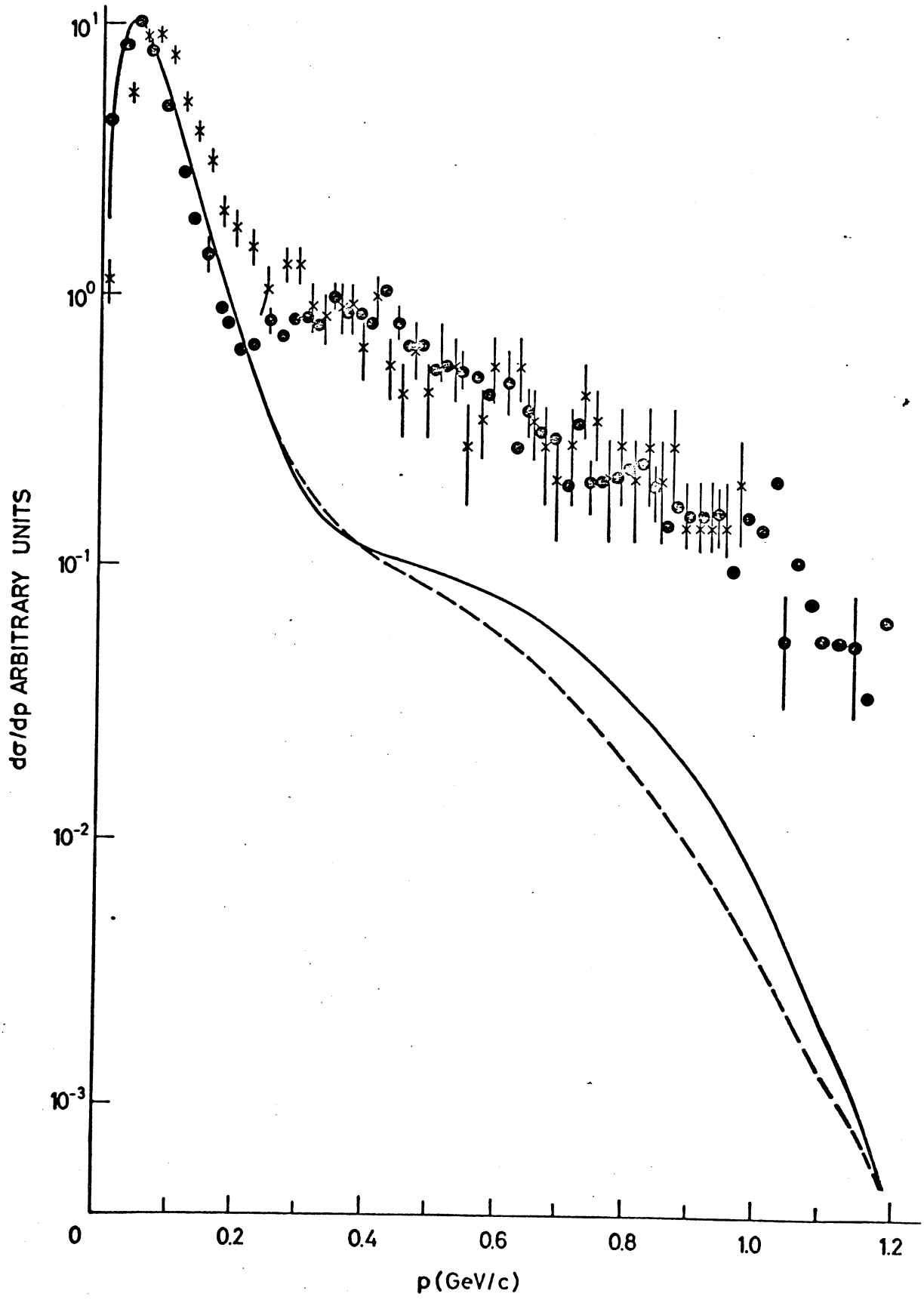
10^1
10^0
10^{-1}
10^{-2}
10^{-3}
0
0.2
0.4
0.6
0.8
1.0
1.2
dσ/dp ARBITRARY UNITS
p (GeV/c)

FIG. 13

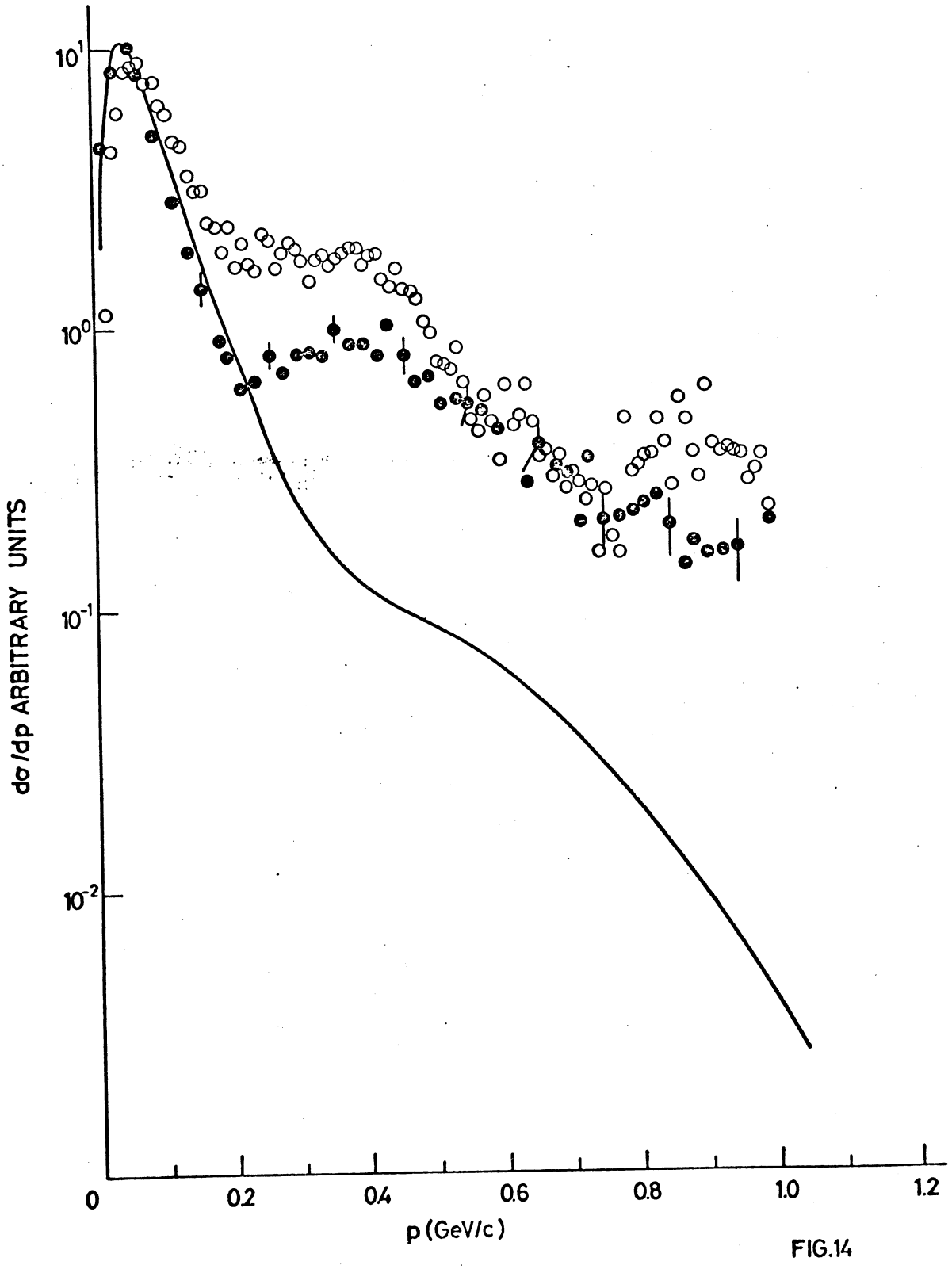

FIG.14

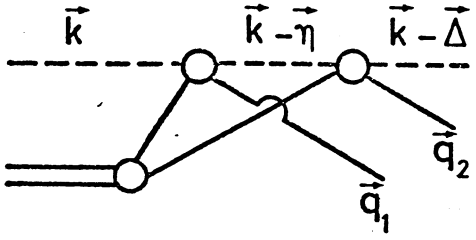
$\vec{k}$
$\vec{k}-\vec{\eta}$
$\vec{k}-\vec{\Delta}$
$\vec{q}_2$
$\vec{q}_1$

(a)

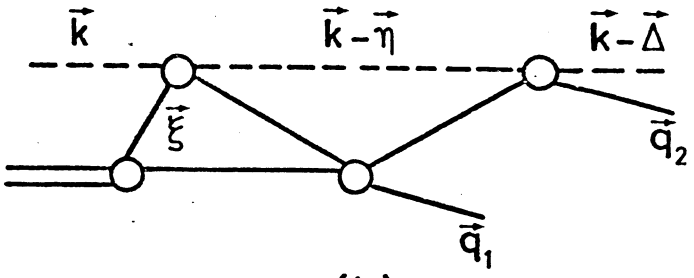
$\vec{k}$
$\vec{k}-\vec{\eta}$
$\vec{k}-\vec{\Delta}$
$\vec{\xi}$
$\vec{q}_2$
$\vec{q}_1$

(b)

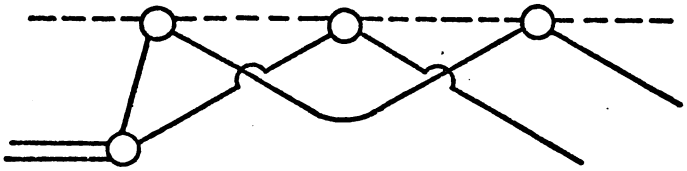

(c)

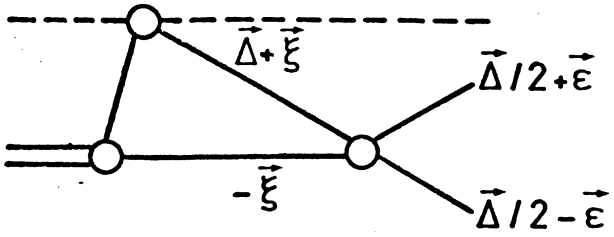
$\vec{\Delta}+\vec{\xi}$
$\vec{\Delta}/2+\vec{\varepsilon}$
$-\vec{\xi}$
$\vec{\Delta}/2-\vec{\varepsilon}$

(d)

FIG.15

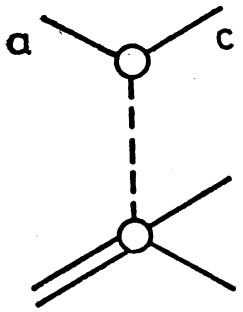

(a)

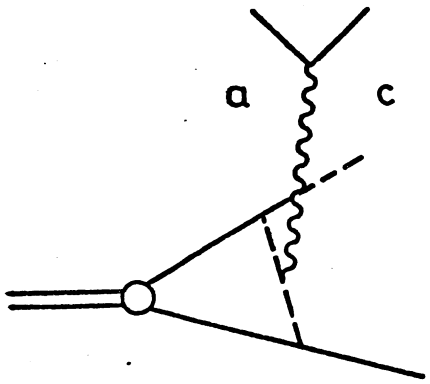

(b)

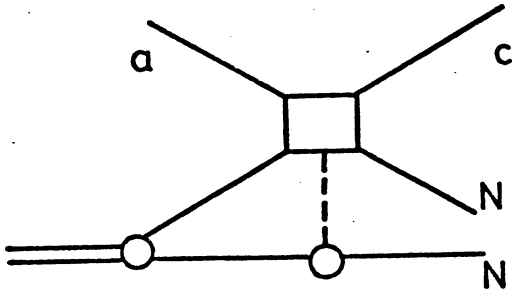

(c)

FIG.16

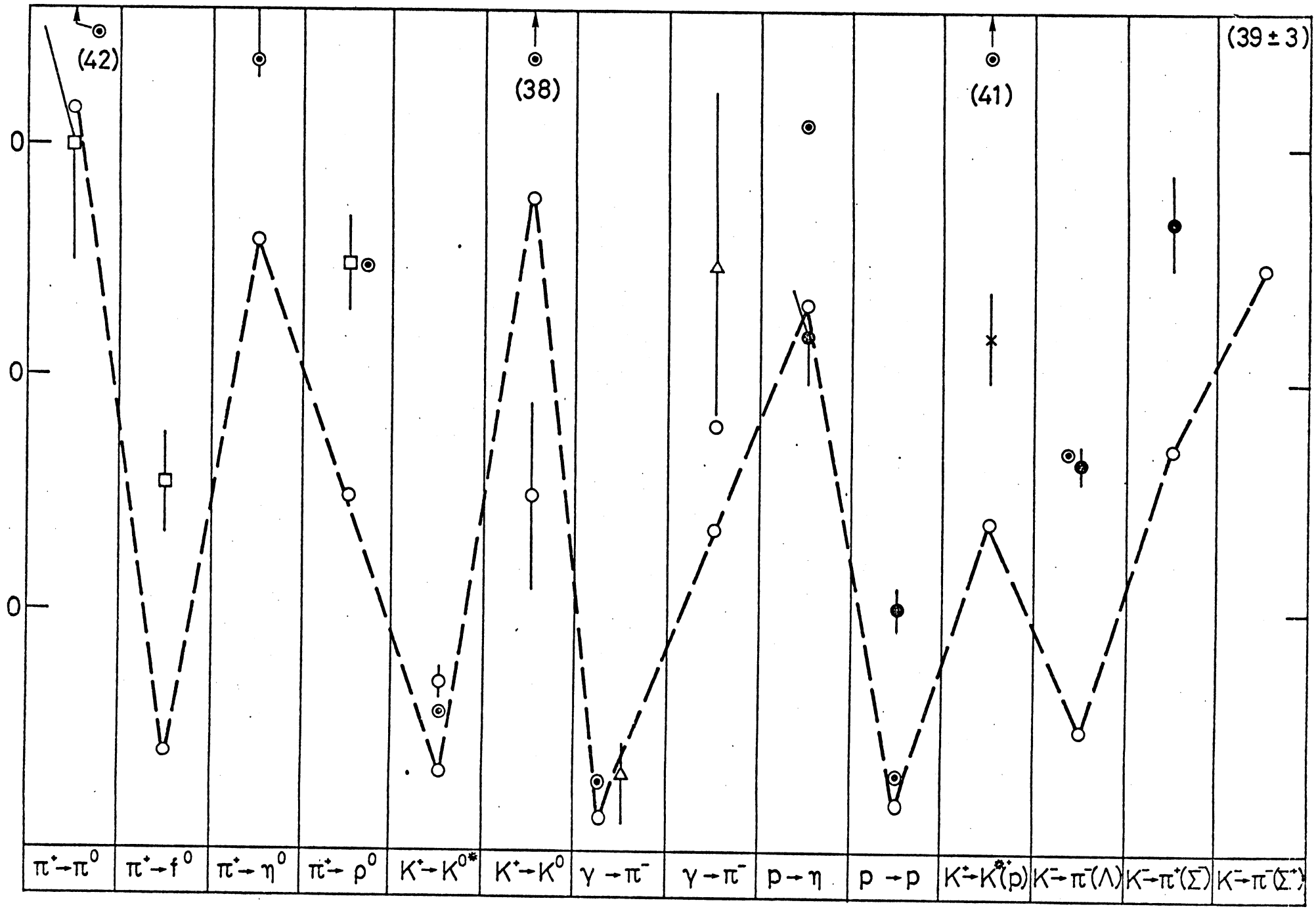
(42)
(38)
(41)
(39 ± 3)
0
0
0
$\pi^+ \to \pi^0$
$\pi^+ \to f^0$
$\pi^+ \to \eta^0$
$\pi^+ \to \rho^0$
$K^+ \to K^{0*}$
$K^+ \to K^0$
$\gamma \to \pi^-$
$\gamma \to \pi^-$
$p \to \eta$
$p \to p$
$K^+ \to K^{*}(p)$
$K^- \to \pi^-(\Lambda)$
$K^- \to \pi^+(\Sigma^-)$
$K^- \to \pi^-(\Sigma^{*+})$

FIG. 17

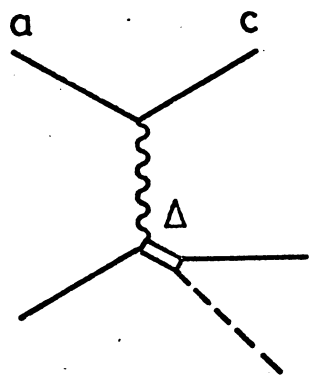

FIG. 18

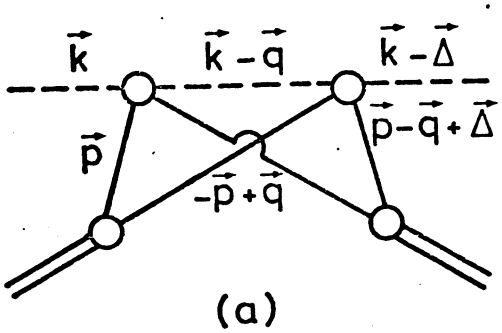

(a)

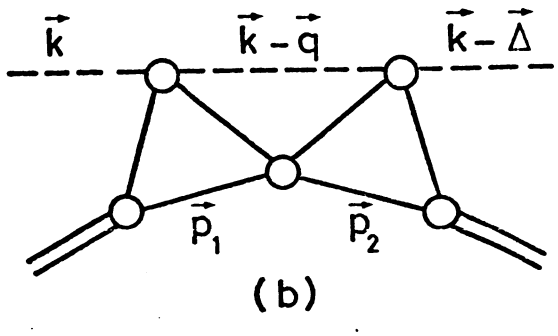

(b)

FIG.19